Universiteit Utrecht

CRODA
Innovation you can build on™

Final Report

2016

Mesoporous ZSM-5 Zeolites as Catalysts for Branching of Unsaturated Fatty Acids

Silvia Zanoni (UU-4202678)

Supervisors:

Sophie Wiedemann

Bas Wels

Prof. dr. ir. Bert M. Weckhuysen

Note that this is not the complete version of the report.

Sensitive information included in the content of this report have been left out, in consideration of the confidentiality agreement that has been signed with Croda, to protect the company and preserve any confidentiality under patent and /or trade secret laws.

Abstract

Isostearic acid (ISAC), a mixture of saturated mono- and poly- methyl-branched C_{18} fatty acids, combines the desirable liquidity of oleic acid with the chemical, oxidative and thermal stability of stearic acid. Hence, it is a highly valuable product for several applications, such as lubricants, cosmetics and personal care. However, ISAC is currently produced as a co-product of the clay-catalysed polymerisation of unsaturated fatty acids, which makes its production limited and costly. As an alternative to the clay, zeolites can be employed, being considerably more selective to the alkyl-chain isomerisation (branching) reaction.

An earlier screening of commercially available catalysts revealed that an H-ZSM-5 […] (henceforth referred to as H-T22) has the highest performance due to its superior selectivity and relatively high activity, compared to other commercial zeolites. However, this catalyst undergoes rapid deactivation and still needs relatively high loading [..] to reach an acceptable activity. This suggests that only a limited depth of the catalyst pore is actively used in H-ZSM-5. Hence, it is hypothesised that increasing the number of active sites accessible to the reactant would enhance catalyst activity. A way to obtain such enhanced accessibility is the introduction of mesopores into the microporous catalyst crystals. This project aims to show that an alternative catalyst could be in fact found in hierarchical zeolites (i.e. with two levels of porosity).

After an extensive literature research, two commercial catalysts with different Si/Al ratio were chosen and subjected to a selection of top-down modification techniques, with the goal of introducing intra-crystalline mesoporosity. Specifically, an NH_4-Z80 with [...] and NH_4-Z23 with [...] were subjected to [...]. The activities of the resulting catalysts toward alkyl-isomerisation of oleic acid were then tested, and their performances compared to that of the reference catalyst, H-T22.

A hierarchical sample was successfully obtained by [...] treatment of NH_4-Z80. This mesoporous catalyst (H-Z80-AT) shows significantly improved conversion compared to its unmodified version (H-Z80-P), outperforming that of the H-T22 catalyst (91% conversion reached after 5.5h reaction time versus 84% obtained with the H-T22 and 35% with the unmodified H-Z80-P). These results demonstrate the potential of hierarchical ZSM-5 zeolites for the production of ISAC, although more in-depth research should be conducted to find a definitive and commercially feasible solution. It is also hypothesised that the reason behind the good catalyst performance of H-T22 lies in its textural properties, i.e. small crystals with inter-crystalline macroporosity, which allow for good accessibility to its high concentration of acid sites.

Contents

1. Introduction

1.1. Project outline

Saturated branched-chain fatty acids (SBFA) derived from (renewable) vegetable oils hold a unique position in the oleochemical industry. Like unsaturated liquid fatty acids, they exhibit good low-temperature liquidity and biodegradability, lubricity and dispersing properties; however, the thermal and oxidative stabilities of SBFA are much superior, allowing them to be used in more demanding applications.

The production yield of SBFA is limited to about 50% or less, as they are currently produced as a co-product in the clay-catalysed polymerisation of unsaturated fatty acids process.[1–3] Hence, finding a more selective route to branched fatty acids is highly desirable, to avoid product balance issues and costly purification processes. Such a solution would lower production costs and potentially open up new markets and applications.

About ten years ago, the prospect of a direct process for the alkyl-isomerisation of fatty acids moved closer when ferrierite (FER), a medium-pore zeolite, was found to be an effective catalyst for the isomerisation of oleic acid (OA).[4] The exceptional properties of this zeolite are due to the ideal size of its 10-membered ring (10-MR) channels and the optimum strength and density of the Brønsted acid sites of the catalyst in its activated acidic form (H-FER). The oleic acid molecule needs to enter these 10-MR channels to reach the Brønsted active sites and undergo alkyl-isomerisation, while oligomers can be formed only on active sites located on the external surface and present in low concentrations in FER zeolites. Therefore, such a combination of structure and acidity allows for high selectivity toward mono-branching while inhibiting oligomerisation. However, recent studies have shown that the reaction is limited to the pore mouths of the 10-MR channels. Initial high catalyst activity is quickly lost due to coke deposits which block pores and deactivate the acidic sites by hydrogen transfer reactions.[5] Hence, only a very small part of the zeolite microporosity is effectively used and, as a result, the catalyst practical life is extremely short, making the catalyst a significant contributor to the overall process costs.[6] A partial solution to this problem is the removal of coke from the catalyst by heat-treatment and consecutive acid washes, which has been reported to allow re-use for up to 20 times (on small scale) with limited loss of activity and selectivity.[7]

ZSM-5, another medium-pore zeolite, is an interesting alternative (although less selective to alkyl-isomerisation than FER) as it is widely available. Specifically, a screening of commercially available catalysts showed a H-ZSM-5 [...] as the best option for fatty acid isomerisation, due to its good selectivity and relatively high activity when compared to other commercial ZSM-5 catalysts. However, this catalyst also undergoes rapid deactivation and still needs relatively high loading to reach an acceptable activity. This again suggests that only a limited depth of the catalyst pore is actively used in ZSM-5, although the exact mechanism of deactivation may differ to that of FER.

By extrapolation from the work done with FER, it is hypothesised that the activity of the ZSM-5 zeolite is restricted to a limited pore depth. Hence, increasing the number of pore mouths accessible to the reactants per gram of catalyst is expected to markedly improve catalyst activity and yield. One option is to increase the external surface area, i.e. reduce the catalyst crystal size; however, this is likely to lead to a parallel increase in oligomerisation (unless modifications are made to remove non-selective sites located at the surface). Another option is to introduce mesopores, to increase micropore accessibility without reducing

significantly the crystal size, hence avoiding a loss in selectivity towards isomerisation in favour of polymerisation reactions. Such techniques have been widely studied and perfected for zeolites like ZSM-5, as reported in literature.[8–14] Furthermore, these mesoporous zeolites have been tested for other reactions involving bulky feedstocks, with good results.

The aim of this project is to review such modification techniques, to select a few of the most promising ones and to test them to confirm the validity of the underlying assumptions. It is hoped that such investigations can result in improvements in the catalyst for the alkyl-isomerisation of unsaturated fatty acids, with equal or higher activity than the currently best performant zeolite.

1.2. Fatty acids and isostearic acid

Fatty acids (FA) are aliphatic carboxylic acids derived from the hydrolysis ('splitting') of triglycerides, the main components of natural fats and oils. The hydrocarbon chain of FA of the most important oils and fats are between C_8 and C_{22}, and generally, possess an even number of carbons. Furthermore, they can be saturated or unsaturated, i.e. with one or more double bonds within their aliphatic straight carbon chain.[15,16] Some commonly-occurring C_{18} fatty acids are reported below, in Figure 1.

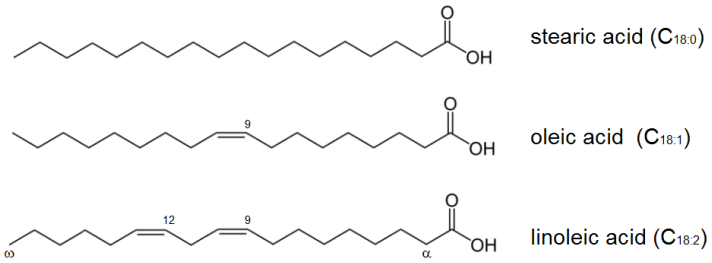

Figure 1: Structure of a few common C_{18} fatty acids. Stearic acid is linear and saturated; oleic acid and linoleic acid are unsaturated, with a double bond in position 9 and two double bonds in position 9 and 12, respectively.

Saturated FA are more stable to oxidation compared to unsaturated acids, making them especially suitable for use in products requiring long shelf life, or in high-temperature applications. However, unsaturated acids have the advantage of better low-temperature liquidity, a characteristic that makes them suitable for certain applications e.g. lubricants and, more generally, easier to store, transport, process and formulate. A modification strategy that results in FA with liquidity *and* excellent oxidative stability, as well as additional desirable properties, is the conversion of linear unsaturated FA to branched-chain saturated FA. Although some branched FA can be found in nature, their sources are not sufficiently abundant or accessible to provide a viable feedstock for industrial scale processes. Therefore, synthetic routes are required to meet the growing demand for branched acids from renewable, plant-based origin. **Isostearic acid** (ISAC), a mixture of saturated mono- and multiple methyl-branched C_{18} FA, is the most important bio-based branched FA currently available, which combines the desirable liquidity of oleic acid with the chemical, oxidative and thermal stability of stearic acid.

However, ISAC is currently produced only as a co-product of the clay-catalysed polymerisation of unsaturated FA (see Figure 2). Clays are two-dimensional layered materials, and fatty acid molecules can enter the interlayers unconstrained, reacting alone or with each other on the active sites to form monomeric (branched), dimeric and trimeric acids. This process was developed in 1957 and brought several advantages compared to the uncatalysed thermal polymerisation employed at that time, namely shorter reaction times and the possibility to use a wider range of feedstocks.[1–3] Initially, the monomeric (unpolymerised) fraction was distilled off from the more valuable polymeric products and sold as cost-effective FA for a range of applications; only about 20 years later, the monomer fraction was characterised in detail and found to consist mainly of unsaturated mono and poly methyl-branched FA.

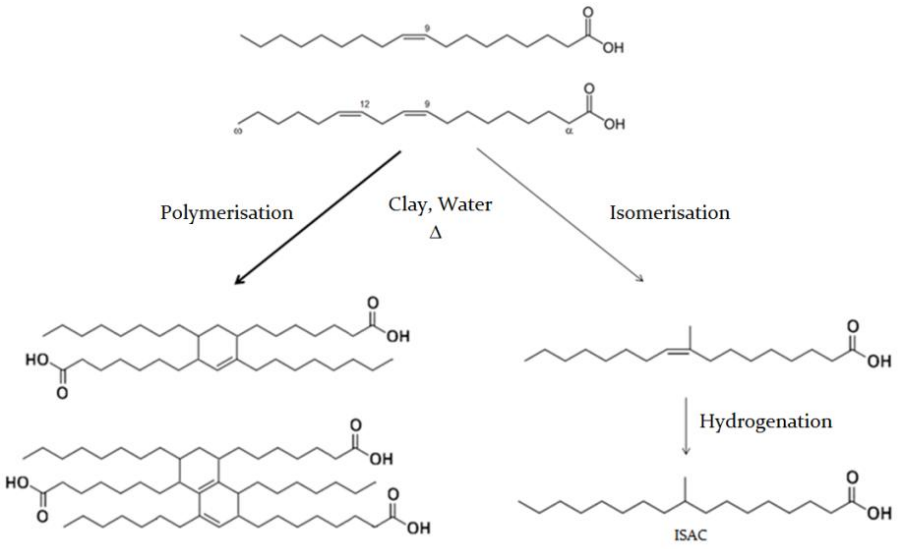

Figure 2: Clay-catalysed polymerisation of commercial oleic acid ($C_{18:1}$), which also contains a small percentage of (polyunsaturated) linoleic acid ($C_{18:2}$). Besides the oligomers produced by the polymerisation reaction (dimeric and trimeric acids, on the left), the products include a mixture of branched monomeric oleic acid isomers; hydrogenation converts the monomeric fraction to ISAC. (Note that all the products here represented contain several isomers).

Later in the process development, this branched fraction was hydrogenated and purified by solvent separation from the saturated straight chain acids, becoming known as **isostearic acid** (ISAC).[17] This mixture of methyl-branched fatty acid isomers possesses qualities that make it ideal for several industrial applications, as reported in the paragraph below. However, the clay-catalysed polymerisation process can be steered only to a limited extent to favour isomerisation. Hence, isostearic acid production is inextricably linked to the polymerised FA demand, and the necessary separation and purification steps make it rather costly. The total availability of ISAC is, therefore, limited and, due to its current production costs, is generally sold only in high value and niche markets. Therefore, in order to meet the faster-growing demand for ISAC, it is essential to decouple the isomerisation from the polymerisation process, so that branched-chain FA can be made in higher quantities and at a lower cost.

1.2.1. ISAC properties and applications

As already mentioned, branched-chain FA display thermal and oxidative stability comparable to that of saturated linear FA, while maintaining the low-temperature liquidity characteristic of unsaturated ones. For these reasons, ISAC is especially suitable for applications and products where high operating temperatures are required, or where a long shelf-life is necessary. The good low-temperature liquidity of ISAC also makes it a good raw material for fatty acid based products used in refrigerated or outdoor environments, such as lubricant esters.[17,18] Interestingly, this low-temperature liquidity is due to the rich mixture of branched isomers, since the pure components have been synthesised and shown to be solid at room temperature. This effect of melting point depression can be explained by the fact that when different branched-chain FA are mixed together, they cannot orient themselves in an orderly fashion within a crystal lattice, whereas a single pure branched fatty acid can pack in a more highly ordered orientation.

ISAC derivatives show good solubility in a wider range of solvents compared to those of the equivalent derivatives of stearic acid. Moreover, ISAC not only has the desired fluidity, oxidative stability and viscosity, but is also non-toxic and biodegradable.

This unique combination of properties among FA makes ISAC industrially useful for a range of different applications. However, due to its relatively high cost of production, it is only used when such properties are essential to the performance of the end product. The main markets of ISAC and its derivatives are lubricants, cosmetics and personal care.

The majority of lubricants are still petroleum-based, although ester-based synthetic lubricants are gaining market share.[18] ISAC is a very suitable fatty acid for the production of ester lubricants, giving products with high thermal stability, low-temperature liquidity, high viscosity index, low toxicity and good biodegradability, all desirable properties.[19] Biodegradable (ester-based) lubricants are especially suitable for outdoor applications, where their unintended release into the environment has limited consequences, unlike many petroleum-based alternatives. Some examples of the application of ISAC in lubricants include metal-working fluids, industrial gear oils, automotive engines, hydraulic fluids, greases and textile lubricants.[20]

A second important application of ISAC (and derivatives) is as emollient and emulsifier for cosmetics and skin care products. They have similar physical properties to those of unsaturated FA, which may be used for such applications, but they offer the advantage of higher colour and odour stability, due to their higher oxidative stability.[21] Furthermore, as with oleic acid, ISAC acts as a carrier and aids the penetration of other substances through the skin.[22] Other applications of ISAC and derivatives in the personal care industry include their use as dispersants for oxides in sunscreen creams and pigments in cosmetics.[23,24]

The above-mentioned applications exemplify a few of the uses of ISAC, and their dependence on its unique properties. However, as stated in the previous section, a cheaper and more direct synthetic route to ISAC is needed, decoupling its production from that of polymerised FA, to allow its potential to be fully exploited.

1.3. Zeolites for the alkyl-isomerisation of fatty acids: an alternative to ISAC production

As evidenced above, the branched structure of ISAC gives it unique and valuable properties. However, expansion of its use in new applications is inhibited by the fact that availability is intrinsically linked to the demand for polymerised FA. Furthermore, purifying the ISAC from the oligomeric fraction by multi-step separation processes adds significant production costs. Although other synthetic routes to branched-chain FA exist, they are based on petrochemical sources and are generally even more complex and costly for the production of equivalent or similar molecules. Therefore, there is a need for a more direct, cost-effective and efficient process for the production of ISAC.

Zeolites, aluminosilicate solids materials with tetrahedrally connected frameworks and very ordered micropores of molecular dimensions, represent a promising alternative to clay catalysts for improved selectivity to branching. Zeolites possess channels and cages large enough to contain extra-framework cations and to permit the uptake and desorption of molecules varying from hydrogen to bulkier organic molecules.[25] The suppression of the polymerisation route is due to the shape selectivity conferred by such a pore structure. The small volume of the pores makes bimolecular reactions very unlikely to occur on active sites positioned inside the pores, limiting the occurrence of such reactions on remaining sites located at the external surface. Furthermore, the ratio between Brønsted and Lewis acid sites, their strength, their distribution and accessibility are also factors driving the reaction towards isomerisation or oligomerisation.

Conceptually, zeolites are based on pure silica frameworks with some silicon ions substituted by aluminium ions. The substitution of Si^{4+} by Al^{3+} imparts an overall negative charge to the framework, which is balanced by the presence of extra-framework cations within the pore space. When the counter ion is a proton, a Brønsted acid site is created (Figure 3a). Therefore, the maximum number of Brønsted sites depends on the Al content. However, the strength of such sites also depends on the global composition of the zeolite framework. In fact, the mean electronegativity, which changes with the aluminium content of the framework, is proportional to the acidity of the hydroxyl bridging sites. Generally, the mean electronegativity increases with decreasing aluminium content. Hence, the higher the aluminium content, the higher the density of Brønsted acid sites, but the lower their strength. Furthermore, the Si–O–Al bond angle, which depends on the zeolite structure type, affects the partial charge and the acid strength of the hydroxyl protons; this means that the composition of the zeolite is not sufficient to determine its acidity.

The second important type of hydroxyl groups in zeolites are the silanol groups (SiOH), which are located on the external surface of crystal particles or at framework defects (Figure 3b,c). Healing of framework defects can occur by silicon migration, formation of silanol groups, or formation of hydroxyl groups at extra-framework aluminium (EFAl) species (Figure 3d).

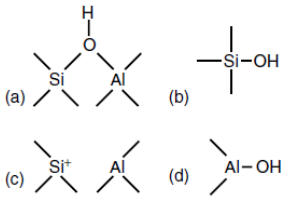

Figure 3: Schematic representation of the different acid sited found in zeolites. a) Brønsted acid site, bridging hydroxyl group; b) silanol group; c) aluminol group; d) defect site.[25]

Therefore, zeolites offer tuneable acidity and shape selectivity in catalysis, making them a promising choice for the alkyl-isomerisation of fatty acids.

The shape selectivity of zeolites has been widely employed for other industrial applications where branching products were needed. An example is provided by the skeletal isomerisation of butene to isobutene. To obtain high yields of isobutene, narrow-pore 10-member ring (10-MR) zeolites are required.[26] Specifically, ferrierite was shown to have the best activity and selectivity for butene isomerisation. Besides the shape and size of the 10-MR channels (4.2x5.4 Å), pore mouth catalysis at the Brønsted acid sites located in these channels was proposed to be the source of its remarkable isobutene selectivity.[27]

These studies provide further evidence that zeolites could also be employed for the alkyl-isomerisation of fatty acids, such as oleic acid (OA). Due to the size of fatty acids compared to butene, the first attempts of zeolite catalysis for oleic acid conversion to branched unsaturated fatty acids were done using a mordenite zeolite. This zeolite presents linear, one-dimensional and larger 12-MR channels (6.5x7 Å), which were thought to be big enough to be accessible by OA, but small enough to avoid dimerisation reactions. However, only considering the pore size is not a sufficient criterion when selecting a catalyst. For example, zeolites with different channel intersections but same pore size can vary in selectivity and activity, due to differences in the ease of reactant and product diffusion. Furthermore, the overall acidity and the ratio between Lewis and Brønsted acid sites are also crucial in determining activity and selectivity of a catalyst and, as mentioned earlier, the factors influencing catalyst acidity are several. For example, in the case of mordenite, it was observed that the addition of a small amount of water to the reaction increased the conversion of OA to 70%. Such an effect was believed to be due to the production of additional Brønsted acid sites.[28,29]

Although other zeolites have been tested for the alkyl-isomerisation of fatty acids, a real breakthrough was made in 2007, when Ngo et al. reported high OA conversion (98%) and selectivity toward branching (85%) by using a protonated ferrierite catalyst (H-FER).[4] Different commercial ferrierite zeolites were tested and highest activity was reported for the zeolites with Si/Al ratio below 15. The composition of the branched-chain FA obtained by H-FER was found to differ from that produced by other Brønsted acid catalysts. Specifically, ferrierite was shown to be highly selective towards mono-branching.[30]

Furthermore, Ngo et al. determined the position of the methyl-branching in the hydrogenated branched-chain FA after conversion to picolinyl esters by GC-MS (further elucidated in later work by GCxGC-TOF-MS analysis[31]).[4] Their initial analyses reported that 84% of branched products by ferrierite had the methyl branch on the 8 to 14 positions, while only 54% of the ISAC from the clay catalysed product had these branching positions.

Further investigations from the same author revealed that the selectivity toward the monomeric fraction could be improved by the addition of triphenylphosphine (TPP).[31,32] This Lewis base is believed to interact with the acidic sites on the external surface of the

catalyst and suppress the formation of fatty acid dimers. Conversely, the acidic sites situated inside the pores remain unaffected, due to the bulkiness of the TPP molecule which prevents it from entering the pores.

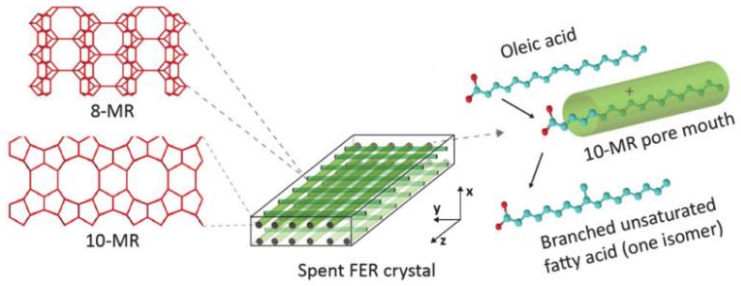

Figure 4: Skeletal isomerisation of OA in the presence of protonated zeolite ferrierite (H-FER); a schematic representation of the spent H- FER crystal is shown at the centre of the figure. The left side of the figure illustrates the framework seen along the [001] plane of the crystal, perpendicular to the direction of the 10-MR pores, and that along the [010] plane, perpendicular to the 8-MR pores direction. The right shows pore mouth catalysis of oleic acid, postulated to control the selectivity of this catalytic reaction.[6]

However, after a very fast initial activity, ferrierite was found to deactivate quickly. This is due to severe pore blockage by coke formation, which is detected already in the earliest stage of the reaction and reaches a constant level within the first minutes, limiting the reaction to the pore mouth of the 10-MR channels of the catalyst (see Figure 4).[5,6] Nonetheless, ferrierite represents the catalyst with the highest activity for the production of mono-branched FA.

1.3.1. ZSM-5 for the isomerisation of oleic acid

Although less selective to branching, ZSM-5, a zeolite with an MFI framework, can also be employed for the alkyl-isomerisation of oleic acid. Its 10-MR pores (5.1x5.5 Å) are slightly larger than the 10-MR ferrierite ones (4.2x5.4 Å), and are intersected by zigzag channels, as depicted in Figure 5, creating a three-dimensional microporous network.

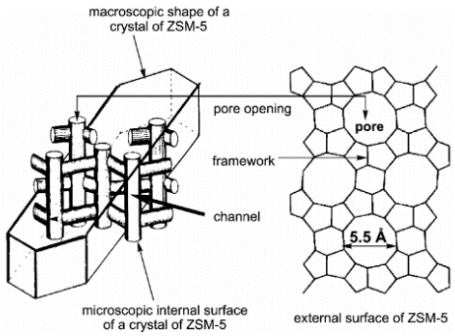

Figure 5: Schematic representation of the crystal shape, pores structure and framework of ZSM-5 zeolite. 10-MR pores (5.1x5.5 Å) are intersected by zigzag channels.[33]

The activity of the best performing ZSM-5 [...] H-T22 is still not satisfactory. As a result, the catalyst makes a major contribution to the process costs and its separation from the product is time-consuming.

Several other commercial ZSM-5 zeolites have been tested for this purpose, but a candidate has yet not been found that meets every requirement. As already mentioned, it is assumed that, due to fast coke formation, the activity of the ZSM-5 zeolite is restricted only to a limited pore depth. Introduction of mesopores should therefore enhance access to the active sites responsible for the isomerisation reaction, while leaving the external surface largely unaffected, thereby avoiding a parallel increase in the polymerisation process.[34] The benefits of mesoporous zeolites obtained by post-synthetic modifications have already been reported for other reactions involving bulky feedstocks.[35–38] Hence, there are reasons to believe that such modifications would also have positive effects on the performance of ZSM-5 in the alkyl-isomerisation of unsaturated FA. The following sections

provide more information on the techniques for the introduction of mesopores to zeolites, i.e. creating hierarchical systems, and their advantages compared to unmodified catalysts.

1.4. Hierarchical zeolites

Zeolites are materials with active sites confined in micropores, generally of molecular size (0.25-1 nm), which enable shape-selective catalytic transformation. Three types of shape selectivity can take place in zeolite catalysed reactions. Firstly, reactants with dimensions larger than the pores are not able to reach the active sites. This is generally referred to as reactant shape selectivity. Secondly, transition state selectivity can occur; if a reactant does reach the active site, only certain transition states are favoured depending on the pore shape, influencing the kind of product that can be obtained. Finally, some generated molecules could still be too large to desorb as a product. In this case, such molecules can either be converted to smaller ones or, if unable to exit, they will block the pores, contributing to the deactivation of the catalyst. This last type is called product shape selectivity.

It is clear that zeolite micropores are beneficial for shape selective reaction, but also impose significant diffusional constraints. The transport of molecules to and from the active site (measured by D_{eff}) is hindered when the site is located inside a pore of diameter close to that of the molecule itself. This represents a major disadvantage, since the catalyst is not utilised to its full potential. The degree of catalyst utilisation can be calculated by the effectiveness factor (η) and depends on the Thiele modulus (φ), a parameter that indicates the ease of diffusion of a molecule through a pore (see Figure 6). In fact, if the diffusion of molecules is too slow ($\varphi \to \infty$ and $\eta \to 0$), only the active sites located at a certain depth of the catalyst is utilised. On the other hand, full use of the catalyst ($\varphi \to 0$ and $\eta \to 1$) represents a situation free of any diffusion constraint.

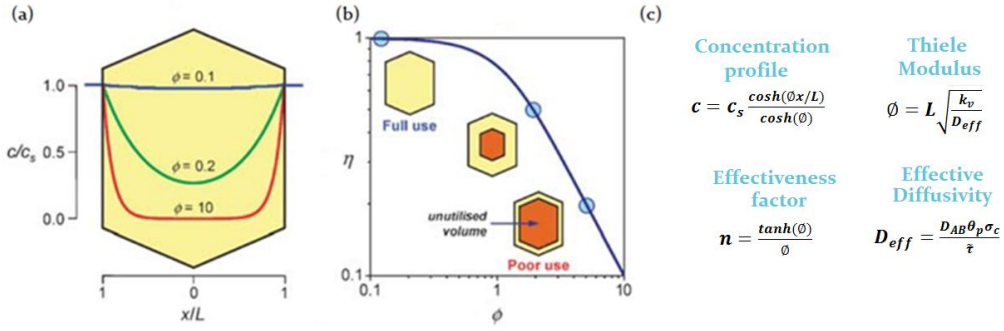

Figure 6: a) Concentration profiles across the zeolite crystal for different Thiele modulus (φ). When φ=0.1, the concentration is practically uniform (c/c_s=1), across the crystal while for φ=10, the concentration is extinguished (c/c_s=0) near the surface. b) Representation of the indirect dependence of the effectiveness factor (η) to the Thiele modulus (φ). Low φ leads to full utilisation of the catalyst, while high φ gives a poor use of the catalyst. c) Relevant equations to the graphs. In the definition of D_{eff}, D_{AB} is the distance between two points A and B within the catalyst particle, θ_p is the porosity of the particle, σ_c the constriction factor and τ the tortuosity of the path that a molecule has to follow to go from A to B. [34,39]

Therefore, to increase catalyst utilisation, a way to lower the Thiele modulus should be found. According to the equation above (φ in Figure 6c) two approaches could be adopted: increasing D_{eff}, which can be achieved, for example, by increasing the width of the pores; or decreasing L, the diffusion path length. The first option is not practical, since zeolites with wide pores (Figure 7b) suffer from low thermal and hydrothermal stability, low acidity and high production costs, in addition to the loss of shape selectivity conferred by the ordered micropores of a standard zeolite. On the other hand, reducing the diffusion path length, while maintaining the microporous system, can give the desired results. Simply decreasing the crystal size can be problematic, as it leads to handling problems, such as difficult filtration of the reaction mixture to remove the catalyst from the product. Another strategy that can be adopted to shorten the diffusion path length in zeolites micropores is the introduction of mesopores. Zeolites with two levels of pore size, i.e. microporosity *and* the additional mesoporosity, are also referred to as **hierarchical zeolites**. This particular class of zeolites combines the shape selectivity typical of microporous systems with efficient mass transfer, made

possible by the presence of mesopores. Ideally, mesopores should be channels running through the entire length of the catalyst crystal, creating an accessible route for both reactant and products. Mesopores can be introduced in different ways and a schematic representation of the different types of hierarchical zeolites is included in Figure 7. For example, when synthesising closely packed small crystals, a second level of porosity is present as inter-crystal voids. Depending on the crystal size, these inter-crystal voids have different dimensions. Specifically, for crystals ranging in size from 100 to 200 nm, mainly inter-crystalline macropores are formed. On the other hand, if crystals smaller than 100 nm are packed together, then inter-crystalline mesoporosity is present (Figure 7c). Furthermore, hierarchical zeolites can be made by supporting microporous zeolite on mesoporous amorphous materials (Figure 7d). Finally, zeolites can also be synthesised with intra-crystalline mesoporosity, i.e. with mesopores within the catalyst crystal (Figure 7d).[34,40]

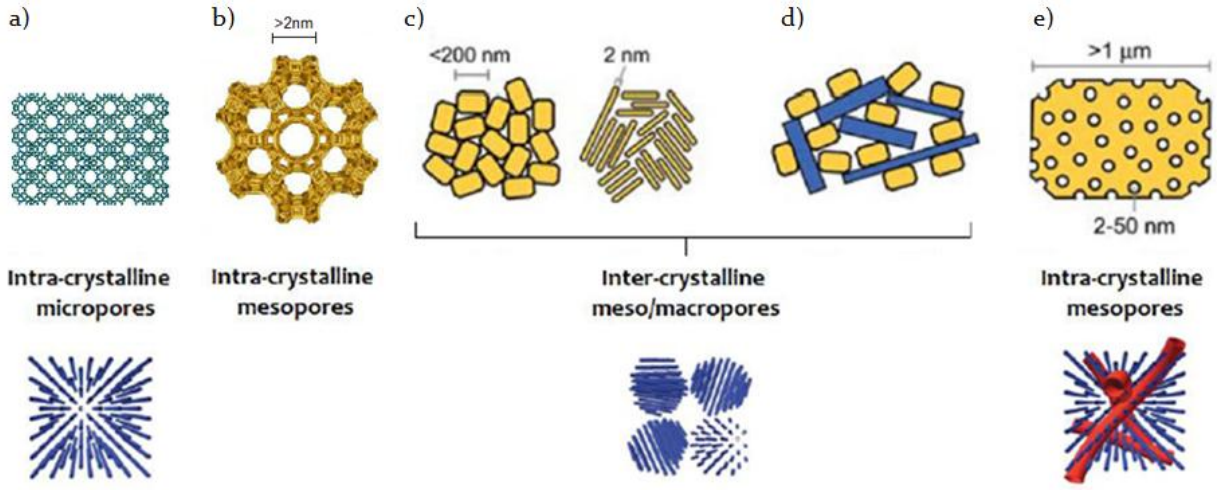

Figure 7: Representation of catalyst crystals with a) intra-crystalline micropore system, with pores of a range of dimensions <2 nm; b) mesoporous zeolite, where the framework is such that ordered pores >2nm in diameter are present within the crystal; c) zeolites small crystals closely packed, having therefore inter-crystalline meso/macroporosity. The voids between these crystals are mainly mesopores when the crystals are nanosized, while macropores are mainly present for crystals of bigger dimensions; d) Supporting zeolite crystals on amorphous mesoporous crystals is another way to obtain inter-crystalline mesoporosity; e) The accessibility to the micropores of the zeolite crystal is enhanced by the presence of mesoporous channels within the crystal itself, giving intra-crystalline mesoporosity. The bottom images give a clearer representation of the different crystalline porous systems. Adapted from [34].

Different strategies have been developed to obtain hierarchical zeolites with intra-crystalline mesoporosity and they can be classified into two main categories: “bottom-up” or “top-down” methods, as depicted in Figure 8.

The most common bottom-up methods make use of templates to introduce mesoporosity to the zeolite. Templating methods can be classified as ‘hard’ or ‘soft’, depending on the nature of the interface between the zeolite crystal and the templating material. Examples of ‘hard’ templates include carbon, $CaCO_3$ nanoparticles or polystyrene microspheres. On the other hand, ‘soft’ templates comprise cationic surfactants or polymers, but also polymeric aerogels, starch and bacteria. Furthermore, assembling protozeolitic units into mesoporous materials with nanocrystalline pore walls and converting amorphous pore walls of mesoporous silicates or aluminosilicates into zeolites are also part of the ‘bottom-up’ category. Other techniques to obtain hierarchical zeolites are classified as ‘top-down’ methods, since they achieve the introduction of mesoporosity by modifying already synthesised zeolites. The most common methods of this category include demetallation techniques, i.e. the selective removal of framework aluminium (dealumination) or silicon (desilication) atoms from a pre-synthesised zeolite. Furthermore, mixed methods are a combination of assembly and demetallation, such as recrystallisation techniques, where the zeolite is partially dissolved and then recrystallised to form mesopores, with the aid of surfactants. Similarly, mesopores can also be introduced in a single-step procedure, where the dissolution of the zeolite is carried on in the presence of the surfactant and crystal rearrangement occurs.[34,41–43]

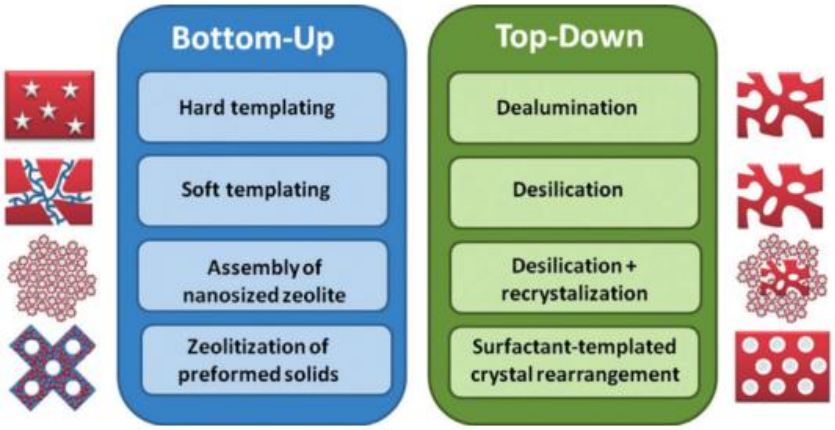

Figure 8: Classification of the techniques to obtain hierarchical zeolites, categorised into the two main "bottom-up" and "top-down" approaches.[42]

For practical reasons, the strategy adopted in this project has been restricted to demetallisation techniques, although all the above-mentioned methods are valid ways to effectively obtain hierarchical zeolites. The literature on demetallisation applied to ZSM-5 is particularly detailed and comprehensive, and the introduction of mesoporosity on this specific zeolite has shown to enhance the activity of the catalyst for a series of reactions. The following is a review of the demetallation methods, including a general introduction on their mechanism and a more detailed summary of the information found in literature about the application of these techniques to ZSM-5 catalysts.

1.4.1. Demetallisation methods

Demetallisation consists in the post-synthetic removal of Al or Si from the zeolites framework. Such techniques take the name of dealumination and desilication, respectively. Dealumination can be obtained in the vapour phase by steaming, or in the liquid phase, by acid leaching, i.e. treatment of the catalyst in aqueous acidic solutions. On the other hand, the removal of Si is achieved by base leaching. The mechanisms of these two modification methods are conceptually different. Therefore, the two treatments are initially considered separately in this section. However, in some cases a combination of the two techniques can be beneficial to obtain optimal mesoporosity; hence, the effect of applying consecutive treatments is also considered in the last part of this chapter. The following paragraphs attempt to summarise the demetallisation mechanism and the impact on crystallinity and acidity of the zeolite brought by these techniques, mainly focusing on the literature on ZSM-5 zeolites. Furthermore, information about the reproducibility and optimisation of such methods is provided, which was essential in planning the methodology for this project.

1.4.1.1. Desilication

Desilication is one of the two demetallisation methods for the creation of mesoporosity and it is generally obtained by treating the zeolite with alkaline solutions. Even though such a technique is more recent compared to dealumination, a lot of research has been done in the past years to investigate and optimise the desilication method by alkaline treatment. In fact, it was shown that for H-ZSM-5 zeolites, alkaline treatment was generally more successful in the introduction of mesopores than dealumination procedures.[8,12] For this reason, an extensive review of the literature on the topic was made, which confirmed alkaline treatment potentials. Based on this review, the main findings on the mechanism and the changes in acidity introduced by the treatment are summarised, reporting the most interesting papers on the matter, specifically on ZSM-5 zeolites. Furthermore, essential information about what are the optimal treatment conditions to obtain mesoporosity and the reproducibility of the technique are also discussed.

Mechanism:

The first investigation of silicon extraction by alkaline treatment was reported for ZSM-5 with the use of a Na_2CO_3 solution under reflux conditions. However, this treatment resulted in an excessive and uncontrolled dissolution of the zeolite, specifically with a preferential dissolution of the interior of the crystals, resulting in hollow crystals.[44] This phenomenon was attributed to a selective extraction of Si and to the presence of an Al gradient within the zeolite particles. In fact, as shown by more recent characterisation studies of large ZSM-5 crystals, the outer surface is often rich in Al, while Si and O are found to be evenly distributed throughout the crystal (see Figure 9).[45] Although these experimental conditions were not ideal to introduce mesopores, these experiments confirmed that preferential Si extraction can be obtained by alkaline treatment, without significantly affecting the Al content.

In 2001, by using milder conditions and NaOH as base, Ogura et al. reported the first evidence of mesopore introduction on a ZSM-5 zeolite by alkaline treatment.[46] The formation of mesopores with a uniform size was observed, while the microporous structure remained unaltered. The catalytic activity for cumene cracking was also tested and revealed to be enhanced by such a treatment. It was therefore confirmed that the alkaline treatment led to an increase in the number of adsorption sites and also in the diffusivity of molecules through the zeolite pores, thanks to the formation of mesopores.

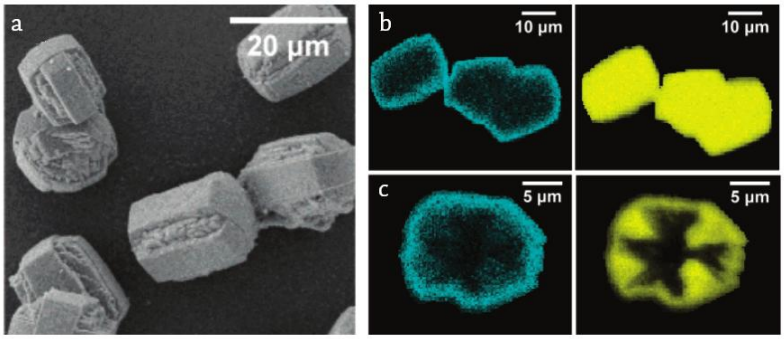

Figure 9: a) SEM micrograph of large crystals ZSM-5; b) SEM-EDX of the non-treated and c) alkaline treated sample. Blue and yellow colours represent Al and Si, respectively.[45]

In the following years after the publication of Ogura et al., Groen et al. investigated thoroughly the introduction of mesopores in ZSM-5 zeolites by alkaline treatment, confirming that controlled desilication induces mesoporosity formation, while preserving the crystallinity of the zeolite.[8,11,45,47–50] They proposed a mechanism for desilication by NaOH solutions, where polymeric silicon-containing species are initially extracted, before disintegrating into smaller entities (see Figure 10).

Furthermore, it has been proposed that realumination might occur as a consequence of alkaline treatment. When large entities are removed by alkaline treatment, they inevitably also include some Al, which is therefore expected to be extracted from the framework. However, analyses of the filtrate after treatment generally reveal very little Al content. The authors suggested that not all the Al removed from the framework remains in the liquid phase, but it is re-incorporated in the solid. This would be due to the consumption of OH^- ions during the progress of the alkaline treatment, which decreases the solubility of Al, which therefore deposited back on the zeolite (see also Figure 16 of section 1.4.1.3).[8]

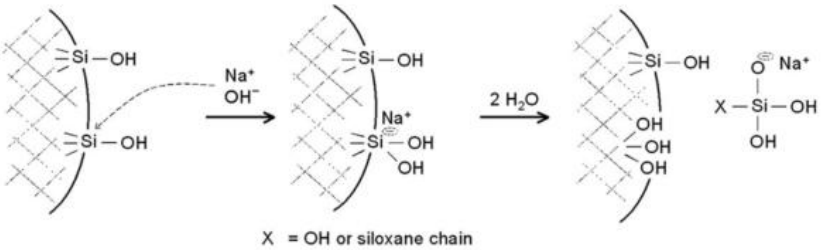

Figure 10: Schematic representation of the removal of silicon-containing species by alkaline treatment with a NaOH solution. Initially, bigger entities are extracted (X=siloxane chain) which are eventually reduced to monomeric species (X=OH).[51]

In addition, Groen et al. investigated the role of aluminium in the desilication mechanism. Specifically, they were able to conclude that the lattice trivalent cation Al^{3+} suppresses the removal of neighbouring silicon species, regulating the alkaline-assisted hydrolysis of silicon towards a controlled mesoporosity development.[45,50] This means that the amount of Al and its distribution in the crystal framework determines the effectiveness of the alkaline treatment. In particular, they established an ideal window of Si/Al ratio (25-50) that the parent zeolite should have to obtain optimal mesoporosity by NaOH treatment, with mesopores in the range of 5-20 nm (see Figure 11). On the other hand, zeolites too rich in Al (Si/Al<15) have only limited mesopore formation when subjected to such treatment, and in zeolites with Si/Al>200 large mesopores and macropores are formed, with a consequent severe loss in micropores content, hence a decrease in active sites concentration.[11,49]

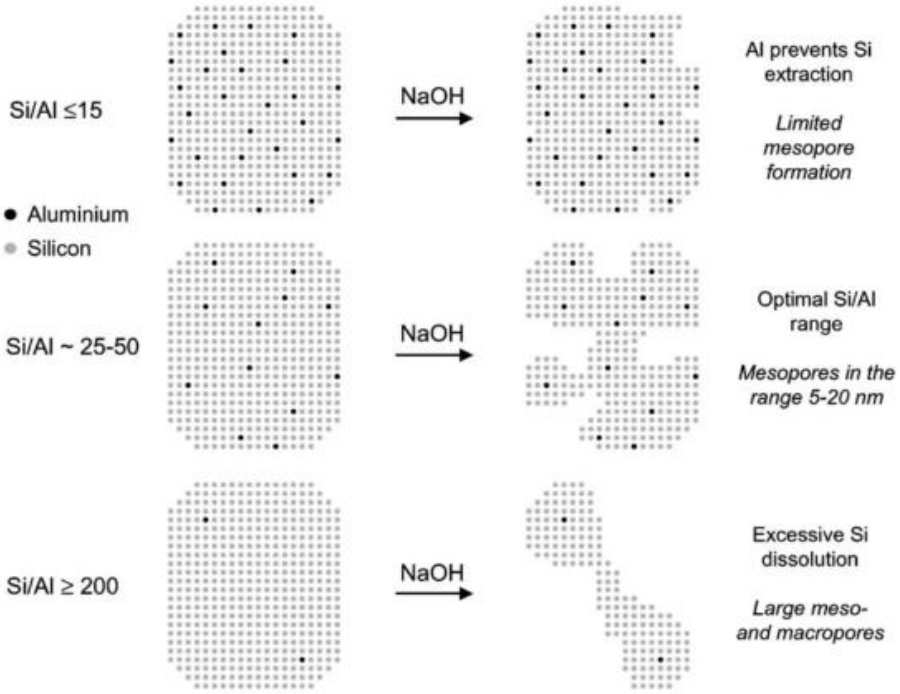

Figure 11: Schematic representation of the influence of the Al content on the desilication treatment of MFI zeolites in NaOH solution and the corresponding typology of pores that are formed.[11]

The improvement of molecular transport properties of mesoporous ZSM-5 obtained by treatment in alkaline solutions was evidenced by Meunier et al., who studied the desorption of isooctane by in-situ diffuse reflectance infrared Fourier transform spectroscopy (DRIFTS).[52] Two samples with markedly different crystal sizes were investigated. The alkaline treatment of the small crystal sample increased the mesopore surface area from 60 to 250 $m^2 \cdot g^{-1}$, while for the large crystal sample the initial 5 $m^2 \cdot g^{-1}$ mesopore area was enhanced to 120 $m^2 \cdot g^{-1}$ by the treatment. Desorption experiments using isooctane evidenced a 4-fold reduction in the characteristic diffusion path length on both hierarchical zeolites, compared to their untreated analogues. Hence, these results confirmed the substantial potential of introducing mesopores also for the improvement of commercial zeolites, generally of small crystal nature, and not only in large crystals where diffusion-limitation problems are more significant.

Schmidt et al. were also able to experimentally show that the presence of mesopores can dramatically increase the rate of diffusion in zeolite catalysts, by studying the elution of *iso*-butane from packed beds of conventional microporous and treated mesoporous zeolite catalysts.[53]

Acidity:

FTIR studies by Bjørgen and co-workers gave further details on the desilication mechanism by NaOH and the influence on the acidity introduced by the treatment. By analysing the υ(OH) region of the FTIR spectra of treated and untreated zeolites, they showed that crystal defects represented by internal Si-OH groups (silanol nests) are removed upon alkaline treatment.[54,55] As shown in Figure 12a, the parent zeolite has five separate bands, which were given the following assignments:

- The sharp well-defined component at 3747 cm^{-1} represents isolated Si–OH groups, which are commonly located on the external surface of the zeolite. This signal is in fact generally perturbed upon adsorption of sterically hindered probe molecules, which are not able to enter the micropore system of the zeolite, and therefore can only affect accessible sites located on the outside.

- Bands with maxima at 3726 and 3692 cm^{-1}, associated with Si–OH sites, predominantly located inside the structure. In fact, unlike external Si-OH groups, they remain unperturbed upon adsorption of large probe molecules. These peaks are normally not observed and the authors believed that their presence was due to the fact that the sample consisted of relatively large crystals. For more common samples with smaller crystals, the contribution of external Si-OH groups is more significant and the peak at 3747 cm^{-1} would be more intense, making impossible to resolve the peaks at 3726 and 3692 cm^{-1}.

- The band located at 3610 cm^{-1}, representing the bridging Al(OH)Si sites, strongly acidic and responsible for the catalytic activity in the alkyl-isomerisation.

- The broad band with a maximum at 3500 cm^{-1} and a shoulder around 3450 cm^{-1} is assigned to a variety of internally located Si–OH sites involved in relatively strong hydrogen bonds, or part of internal defects in the framework.

Upon NaOH treatment, the 3747 cm^{-1} band increases in intensity, whereas the lower frequencies broad band vanishes, implying that after treatment the defects become parts of mesopores, effectively appearing as an ordinary external surface with isolated Si–OH sites represented by the band at 3747 cm^{-1}(see Figure 12b,c). The enhancement of the 3747 cm^{-1} band could also be due to a reduction of crystal size, but this hypothesis was excluded by SEM images, which showed no change in crystallite size of the treated samples.

Furthermore, the NaOH treatment seems to generate EFAl species, which give rise to the rather small component at 3663 cm^{-1}, clearly seen for the treated samples spectra.

Similar results were also obtained by other authors, such as Gil et al., who investigated the differences in the desilication mechanism between ZSM-5 and ZSM-12.[56]

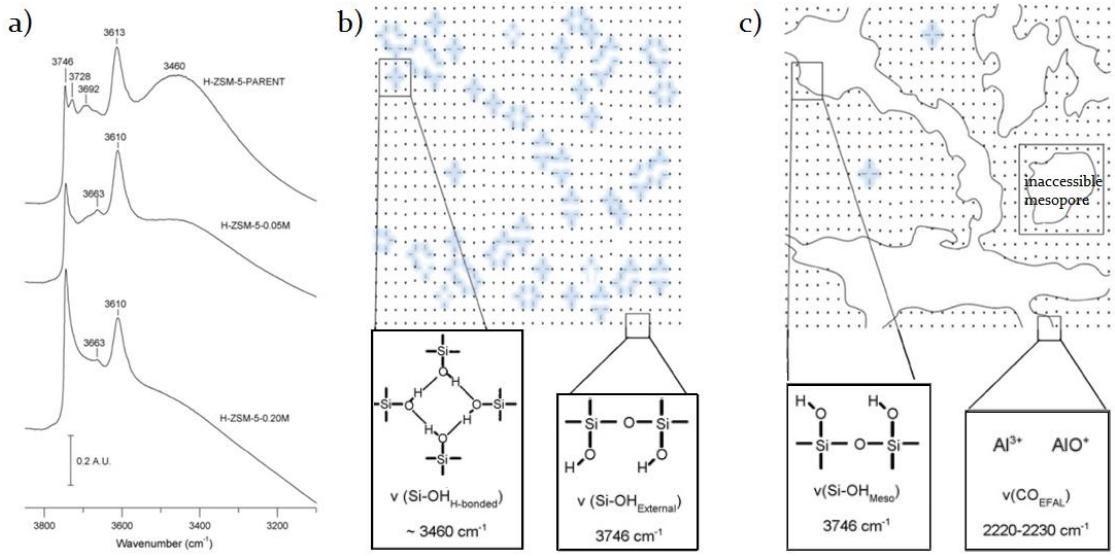

Figure 12: a) υ(OH) region of FTIR spectra recorded at room temperature of a ZSM-5 zeolite (parent, treated in 0.05 M and 0.2 M NaOH solutions. b) and c) represent a schematic illustration for the formation of mesopores, as a consequence of preferential framework dissolution near crystal defects. The species corresponding to specific FTIR signals are also highlighted. For the $\upsilon(CO_{EFAl})$ in c) two species of those that have been proposed in the literature are reported.[55]

FTIR analyses were therefore used to follow the major changes in OH groups resulting from the alkaline treatment, while further tests with probe molecules were used to investigate the changes in acidic strength, active sites location and accessibility introduced by the presence of mesopores. FTIR analyses using CO as probe molecule revealed that the acid strength of the Si(OH)Al Brønsted sites, was virtually unaffected by the alkaline leaching procedure. These results were both confirmed by Holm et al. and Gil et al.[55,56] However, Bjørgen and co-workers also observed a rather weak component at 2220-2230 cm^{-1} in the spectrum of the treated sample (with 0.20 M NaOH), which wasn't present in the spectrum of the parent catalyst, and only barely visible for the mildly treated sample (with 0.05 M NaOH). This band was attributed to CO adsorbed on strong Lewis acidic sites associated with extra framework aluminium created by dehydroxilation during alkaline treatment.[54,55] Note that the adsorption coefficient of CO on these Lewis site bands is very low, making it difficult to quantify such acidic sites with this band. In fact, Gil et al. were not able to observe this band in the spectra of their desilicated samples, while only the band at 2180 cm^{-1} corresponding to the intrinsic Lewis site of the catalyst was present.[56] In order to acquire information on the location and accessibility of the acid sites, Bjørgen and co-workers used a sterically hindered molecule, collidine. For the modified zeolite, only Si-OH on the external surface could be accessed immediately by collidine, while part of these sites located in the mesopores was not reached. The authors hypothesised that some mesopores might be located inside the microporous system, with no access from the outside of the particle by bulky molecules such as the probe employed. Furthermore, experiment of CO adsorption after saturation of the sample with collidine resulted in spectra where the band at 2220-2230 cm^{-1} assigned to Lewis sites vanished, meaning that such sites are reachable by collidine; hence, the Lewis sites created by alkaline treatment must be located at the external surface of the desilicated sample, or at the mesopores surface.[54,55]

Millina et al. also investigated the effect on ZSM-5 acidity caused by alkaline treatment by IR analysis of chemisorbed pyridine.[12] Alkaline treated zeolite showed a negligible reduction in the concentration of Brønsted sites for NaOH concentrations up to 0.3 M. Furthermore, evaluation upon increasing the temperature of desorption of pyridine revealed that the strength of the Brønsted sites was also similar in both parent and modified sample. On the contrary, too aggressive treatments resulted in a loss of acid sites concentration and strength. Again, increased amounts of Lewis acid sites were evidenced for the alkaline treated samples. Specifically, the concentration of Lewis sites was found to be directly proportional to the mesopores surface area. This dependence agrees with the observations of Bjørgen and co-workers, who suggested that the Lewis sites were predominantly

located at the external or newly created mesopore surface, based on the accessibility of Lewis sites to collidine.[55] Similar results on IR studies of pyridine sorption were also obtained by Gil et al.[56]

Treatment optimisation:

The previous paragraphs gave evidence that, for the scope of this project, desilication by alkaline treatment is definitely a valid option to modify commercial catalysts. Therefore, in order to minimise the amount of testing, it is necessary to choose wisely the specific conditions at which each sample should be treated to obtain optimal results. Groen et al. have been studying the matter widely for ZSM-5 and a summary of their findings is graphically reported in Figure 13.[57]

As already explained earlier, Al has a directing role in the formation of mesopores when treating zeolites in alkaline solutions and, for this reason, catalysts with a **Si/Al ratio** ranging between 25 and 50 were established to contain an optimal amount of Al for mesopore introduction. The effect of treating ZSM-5 zeolites with different Si/Al ratio is represented in Figure 13a.

Regarding the treatment **temperature**, it was shown that below 318 K no distinct change in the porous properties can be observed. On the other hand, above 318 K extra porosity starts to develop and the pore volume increases, whereas the mesopore size distribution broadens and shifts to a larger average pore size. [11] As confirmed from Figure 13b, for temperatures above 340 K the surface mesoporosity is no longer increasing. On the contrary, it is reduced, due to the excessive dissolution of the catalyst. Therefore, the optimal temperature for the alkaline treatment was set at 338 K.

As with increasing temperature, increasing treatment **times** up to 30 minutes result in an almost constant increase of surface mesoporosity, while prolonging the treatment for even longer reduces the efficiency of the treatment (see Figure 13c).

Different **alkaline media** were also tested and NaOH showed to be the best option when compared to equivalent solutions of KOH or LiOH (Figure 13d). When basic solutions like NaOH are used to treat zeolites, the zeolite is transformed into its Na-form. Since the active zeolite for the alkyl-isomerisation is H-ZSM-5 (i.e. with H^+ as counteraction, rather than Na^+), the alkaline treated samples need to be exchanged back to the NH_4-form and then calcined. Such procedure would, in fact, allow restoring the zeolite to its active H-form (see also methods section 2.2). This procedure is quite time-consuming, therefore one might think that a solution would be employing NH_4OH to desilicate the samples, which would, in theory, allow direct calcination of the sample after the desilication treatment. However, as it is also shown in Figure 13d, treatment with NH_4OH would not introduce mesoporosity. Hence, this option cannot be considered.

Zeolites are also provided commercially with different **counter-cations**, such as NH_4, Na^+, or already in the active H-form. From Figure 13e, it is clear that the specific counteraction of the samples does not affect the efficiency of the alkaline treatment.

Another factor that was investigated by Groen et al. was the influence of the stirring speed in the efficiency of the treatment. As shown in Figure 13f, above a 200 rpm threshold, the speed at which the catalyst-alkaline solution mixture was stirred had little influence on the mesopore formation.

All the experimental results which are reported in Figure 13 were performed with an **alkaline solution** at a **concentration** of 0.2 M, considered by Groen et al. as optimal. Millina et al. also investigated the effect of enhancing the severity of the treatment by increasing the alkaline solution concentration, with the scope of examining the effect on ZSM-5 acidity.[12] They verified that the concentration of Brønsted acidic sites was not significantly affected up to concentrations of 0.3M. On the other hand, more aggressive treatment with solution having concentration above 0.3 resulted in a lowered Brønsted acidity, due to the excessive dissolution of the catalyst. In a more recent study by the same authors, the methanol to hydrocarbon conversion efficiencies of hierarchical ZSM-5 catalysts was investigated. Specifically, samples treated with NaOH solution at 0.1-0.3 M concentrations for 30 minutes were found to show better activity and longer catalyst life time.[58]

Other authors came to similar conclusions regarding the optimisation of this modification method. A summary table of all results can be found in Appendix 8.1, specifically reporting the data on physisorption analyses and acidity measurement by IR spectroscopy or NH_3-TPD.

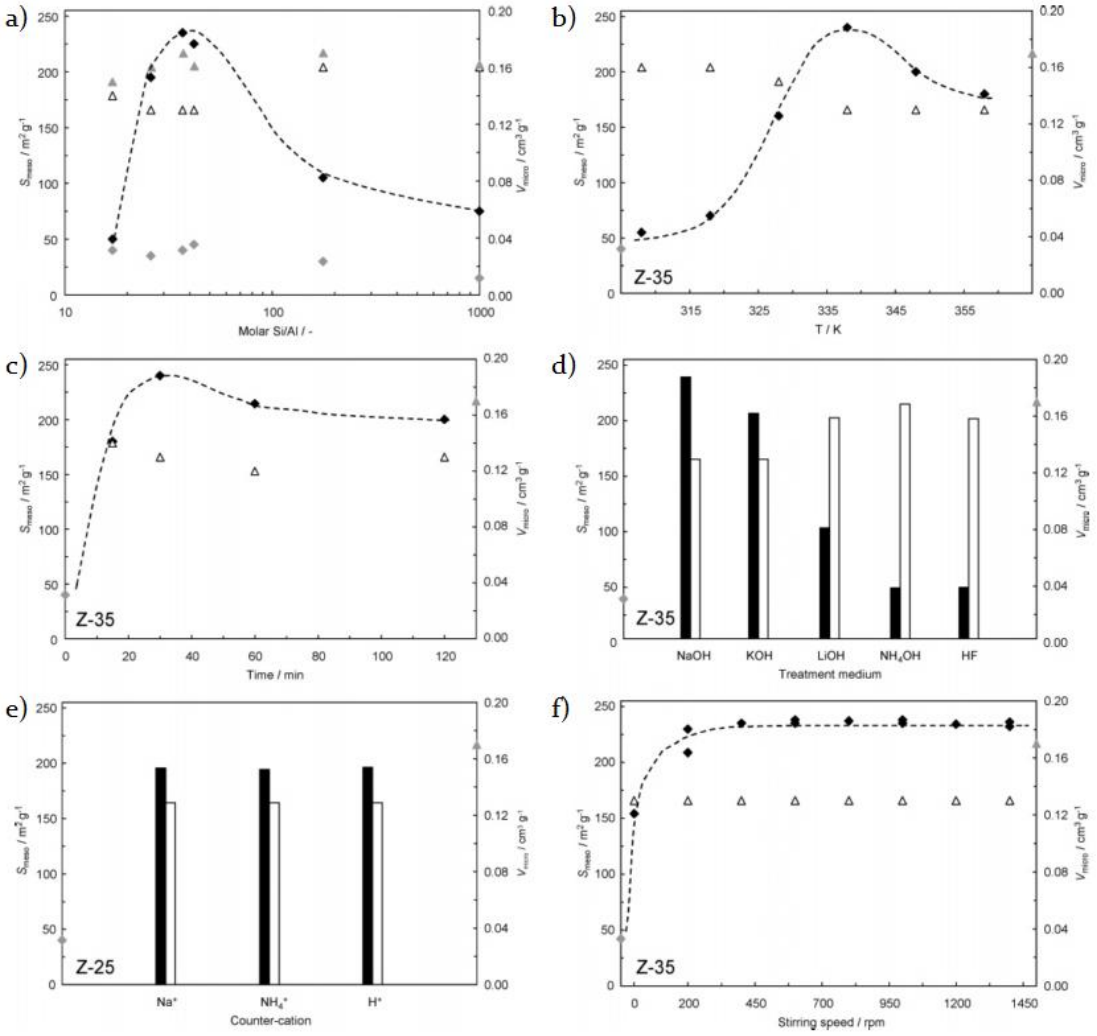

Figure 13: Graphical summary of the effect of different parameters on the introduction of mesoporosity in zeolite ZSM-5 samples. Specifically, the S_{meso} values are plotted against a series of parameters, while maintaining other parameters constant: a) Si/Al ratio; b) temperature; c) treatment time; d) type of alkaline medium, compared to the effect of treatment in HF; e) zeolites with different starting counteractions; f) stirring speed.

It would be preferable to do a screening of modification conditions and test the resulting samples in order to establish their effect on the catalyst activity. However, because of time constraints, the conditions commonly recommended in literature were used to demonstrate the advantage of introducing mesoporosity for improving the alkyl-isomerisation of oleic acid process, although we recognise that these are not necessarily the optimum parameters for this specific reaction.

Reproducibility of modifications:

It is clear that the framework Si/Al ratio impacts greatly the efficiency of the alkaline treatment. Furthermore, there are specific conditions that allow for the formation of optimal mesoporosity, as seen in the previous paragraph. Due to the restricted time available for this project, it was not possible to repeat experiments a sufficient amount of times to test the reproducibility of the methods employed. However, reproducibility studies were found in literature which show that mesoporosity can be introduced to different commercial zeolite samples with same Si/Al ratio within a relative margin of error of 3% when the same treatment

conditions are employed (see Figure 14). Therefore, the results obtained in this project are assumed to be within this margin and repeatability experiments were not prioritised.

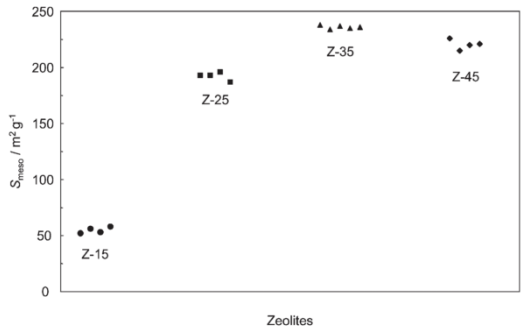

Figure 14: Reproducibility of the alkaline treatment in introducing mesoporosity (mesopore surface area) on different commercial zeolite samples.[11]

1.4.1.2. Dealumination

Mechanism:

The most common way to create mesopores in zeolite on an industrial scale is by steaming, generally at temperatures above 500°C. When in contact with steam, the Al-O-Si bonds hydrolyse and the aluminium is expelled by the framework (generating extra-framework aluminium, EFAl), leaving a vacancy (hydroxyl nest), or causing local amorphisation of the framework. The amorphous phase contains Si mobile species, which can migrate to the voids left by the leaving Al. However, not all vacancies are filled and some of them grow to form mesopores.[59] This mechanism is represented in Figure 15.

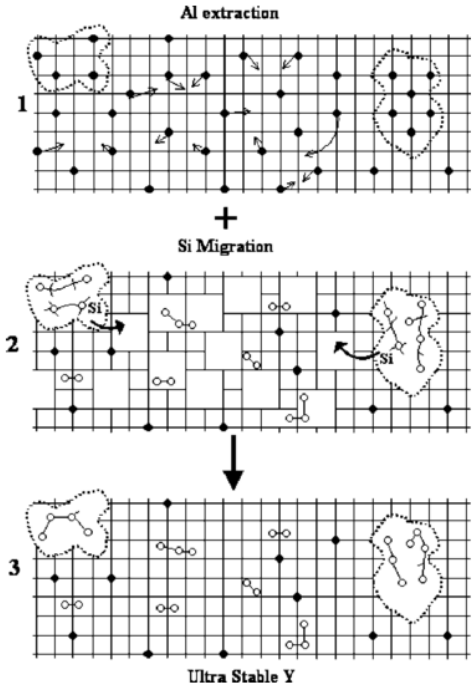

Figure 15: Schematic representation of the formation of mesopores by steaming. The grid represents the zeolite framework; the black dots are Al atoms of the framework, while the open circles represent the extracted Al atoms. The dotted lines indicate the mesopores.[59]

The partial amorphisation represents a disadvantage of this technique, since it leads to a decreased crystallinity, hence a decreased amount of active phase. Furthermore, the fact that part of the formed mesopores is filled with this amorphous debris makes the active sites of the blocked area inaccessible. For this reason, sequential mild acid leaching can be performed to

remove the amorphous material. However, direct acid leaching can also be used to create mesopores. For this purpose, the treatment is generally more severe compared to the acid wash that can be performed after steaming.

Müller et al. compared the effect of dealuminating ZSM-5 samples with oxalic acid and $SiCl_4$.[60] Generally, they observed that samples with larger external surface area were dealuminated more easily, especially in the case of treatment with $SiCl_4$. This is due to the bulkiness of the acid molecules which, combined with the size of the mesopores, allowed for dealumination of the external surface of the samples only. However, the authors claimed an advantage in the use of $SiCl_4$, related to the possibility of healing the sample. Specifically, the silicon atoms of $SiCl_4$ can directly replace the extracted aluminium ones. In this way, no new hydroxyl nests would form and even pre-existing defect could be healed with this treatment. However, except for the change in BET and external surface area, the authors don't provide any information about the introduction of mesopores. In fact, they postulated that the treatment was supposed by them to only affect the external surface of the catalysts.

You et al. investigated the effects on xylose dehydration by post modifications of ZSM-5. They found that treating a ZSM-5 commercial catalyst would not change the textural properties of the zeolite significantly.[61] The only exception being for a high concentration of HCl (3.0 M). In fact, with concentration up to 2.0 M, the physisorption analyses revealed no change in microporosity, external surface area or mesoporosity of the samples, when compared to the untreated one. Furthermore, the relative crystallinity of these dealuminated samples showed to increase, as a result of the removal of extra-framework aluminium species. When testing the effect on xylose dehydration, they obtained an improved selectivity toward furfural, although the conversion was not higher compared to that reached by the untreated sample. On the other hand, harsh treatment with acid at a concentration of 3.0 M was established to decrease both crystallinity and textural properties, due to amorphisation and consequent blockage of both micro and mesopores. Therefore, their results confirmed that acid treatment, if not too aggressive, can be useful for the removal of EFAl when such species are not favourable for achieving a given selectivity. However, this treatment does not introduce significant mesoporosity.

The same results were also observed by Groen et al. when screening the effect of steaming in different Si/Al ratio ZSM-5 samples. It was evidenced only a slight increase in the mesopore surface area, which decreased for zeolites with higher Si/Al ratio. Obviously, a smaller concentration of extractable framework Al results in a lower mesopore area.

Acidity:

It is well known that the Si/Al ratio influences zeolites properties, such as concentration and strength of Brønsted acid sites, catalytic activity and selectivity. Silicon is always present in large majority compared to Al; therefore, removing aluminium from the zeolite framework is expected to have a great impact on the Si/Al ratio, hence on the zeolite acidity. Literature data on dealuminated zeolites confirm that this is indeed the case.

For the steamed samples of commercial ZSM-5 analysed by Groen et al., NH_3-desorption profiles revealed the total acidity to be dramatically decreased, and FTIR measurements confirmed decreased Brønsted sites concentrations, as a consequence of the migration of framework Al to extra-framework positions.[10] On the other hand, the mild acid treatment was shown by You et al. to not leach excessive quantities of Al, but instead remove the EFAl species, decreasing Lewis acidity of the catalyst, while maintaining the concentration of Brønsted sites.[61]

Due to these general limitations, a dealumination technique as steaming is not the best choice to introduce mesoporosity in zeolite catalysts, since it results in an excessive extraction of Al to extra-framework positions and a loss in crystallinity due to amorphisation of the crystal phase, with consequent blocking of the so-obtained mesopores, and reduced Brønsted acidity. However, a mild acid leaching could be beneficial, as it does not result in amorphisation of the catalyst crystals, or in a loss of

Brønsted acidity. Specifically, it can be employed as a method to decrease Lewis acidity, to shift a reaction toward a given selectivity, as it can be efficient in removing EFAl. Since Lewis acids are generally active sites for oligomerisation reaction of oleic acid, this technique could be efficient for tuning the selectivity of the alkyl-isomerisation reaction toward branching. As it is discussed later, this technique can also be applied as a post-treatment following desilication.

1.4.1.3. Consecutive treatments

Dealumination followed by desilication:

In the previous sections, it has been discussed that dealumination might not represent a valid treatment for the introduction of mesopores in ZSM-5 catalysts, while hierarchical zeolites can be successfully obtained with desilication by alkaline treatment. Furthermore, several studies have shown that to obtain optimal mesoporosity, the selection of the parent zeolite should be restricted to those with a Si/Al ratio between 25 and 50, due to the directing agent role of Al. To obtain sufficient mesoporosity in zeolites with low Si/Al ratio, a good strategy could be to first dealuminate the sample, which would increase the framework Si/Al ratio to a more favourable range (25-50) and subsequently treat the obtained catalyst in alkaline solutions. However, besides the concentration of framework trivalent Al species, also species in extra-framework positions can influence the efficiency of the treatment, specifically impeding silicon extraction. These species are generally found in steamed or acid leaches samples. Therefore, performing a dealumination on a low Si/Al sample, prior desilication, would not bring the desired effect. On the contrary, the extra framework aluminium created by dealumination treatment would decrease mesoporosity formation, even if the framework Si/Al ratio had been enhanced by the treatment. A solution would be to remove these extra-framework species, prior to desilication, by mild treatment with chelating agents, such as oxalic acid. In Figure 16 the effect of alkaline treatment, steaming and subsequent alkaline treatment and of steaming, followed by first oxalic acid wash and then alkaline treatment are schematically represented.

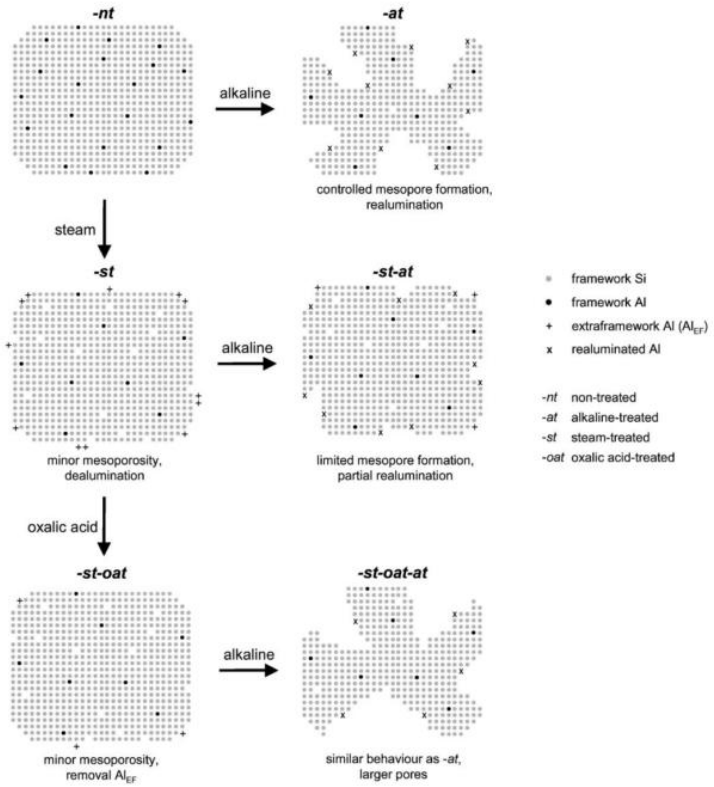

Figure 16: Schematic representation of the effect that subsequent treatments have on the introduction of mesoporosity in zeolites, proposed by Perez-Ramirez and co-workers.[8]

As already explained, desilication is impeded by the EFAl created by steaming. Several other studies also report that alkaline treatment following steaming did not bring mesoporosity to zeolites samples. However, by removing EFAl species by a mild oxalic acid treatment the susceptibility to desilication can be restored. This tactic leads to formation of larger mesopores due to the enhanced Si/Al ratio in the acid-treated zeolite, when compared to the solely alkaline treated sample.[8]

Desilication followed by acid wash:

Another interesting combination of treatments that was investigated was a desilication by alkaline treatment, followed by a mild acid wash with inorganic acid solutions at low concentrations. As already mentioned in the dealumination section, a non-aggressive acid wash can be useful to remove extra-framework species, reducing the Lewis acidity of the catalyst.

Peréz-Ramiréz and co-workers defined this technique as ideal in the introduction of mesopores in zeolites with low Si/Al ratio, since desilication alone was by them established to not work efficiently on such zeolites. According to them, desilication of the Al-rich zeolites would result in a parallel removal of Al species from the framework, which would partially block the access to the catalysts pores. The subsequent acid treatment would remove the amorphous Al-rich debris found in the alkaline treated sample and result in more accessible active sites. This concept is schematically represented in Figure 17. Despite promoting this method as particularly useful for ZSM-5 zeolites with low Si/Al ratio, its application to zeolites with higher Si/Al ratio can also be beneficial.

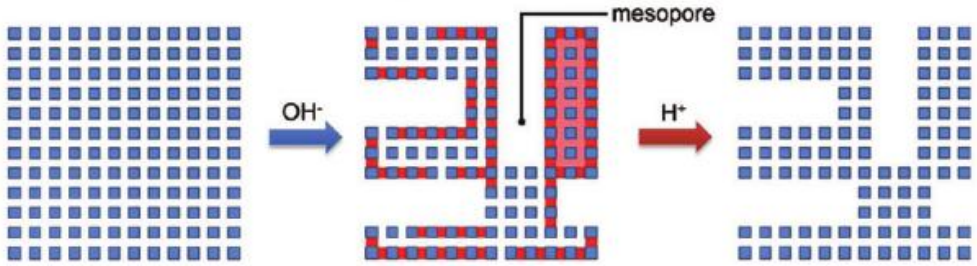

Figure 17: Schematic representation of the micropore blockage by Al-rich debris on the external surface upon alkaline treatment and the removal of such debris upon subsequent acid wash treatment.[14]

For example, Millina et al. investigated the effect of these subsequent treatments on a ZSM-5 commercial catalyst with a Si/Al ratio of 40.[12] The samples that were subjected to acid wash after alkaline treatment exhibited similar or slightly decreased Brønsted acid concentration to that of the lonely alkaline treated sample. However, the acid-washed samples showed substantially reduced Lewis acidity and consequently a lower total amount of acid sites per gram. Furthermore, an enhanced volume of micropores was measured for the samples which received the acid wash, post alkaline treatment. This could be associated with the removal of the extra-framework species that might have been blocking the access to the micropores in the alkaline treated samples (see Figure 17). This demonstrates the potential utility of the acid treatment to improve the active site efficiency of hierarchical zeolites obtained by desilication with alkaline solutions.

The work from Dapsens et al. is an example that removal of Lewis acidity by acid wash might not always be beneficial.[62] In their studies, the modification of ZSM-5 catalyst was tested with the aim of improving the conversion efficiencies of dihydroxiacetone isomerisation to lactic acid. In this case, Lewis acidity is needed. Therefore, among the samples made by them, those that were only treated with alkaline solutions showed a better performance than those who received also an acid wash as a post-treatment, which Lewis sites concentration had been lowered.

On the contrary, xylene isomerisation selectivity can be improved by removal of Lewis acid sites, as showed by a study by Fernandez et al.[35] Again, extensive mesoporosity in ZSM-5 was introduced by controlled silicon leaching with NaOH. However, the treatment also induced substantial aluminium redistribution, increasing the density of Lewis acid sites located at the external

surface of the crystals. Therefore, although the mesoporous zeolite displayed a higher o-xylene conversion than its parent, owing to the reduced diffusion limitations, the selectivity to p-xylene decreased, and fast deactivation due to coking was observed. As could be expected, a consecutive mild HCl washing of the hierarchical zeolite proved effective to increase the p-xylene selectivity and reduce the deactivation rate.

1.5. Selected choices for ZSM-5 modification

The previous section gave a comprehensive review of techniques for the introduction of mesopores by demetallisation. Not only the mechanism of such techniques was discussed, but also an overview of the screening of procedures for the optimisation of the method was provided, specifically for the introduction of mesopores in ZSM-5 catalysts. Such literature data were used to make a selection of the appropriate methods to obtain hierarchical ZSM-5. The mesoporous samples obtained by modifying commercial catalysts with the selected methods were then tested for the alkyl-isomerisation of oleic acid. Their performance was compared to H-T22, to prove that hierarchical zeolites would be suitable for fatty acid isomerisation.

Ideally, it would have been interesting to modify a wider range of commercial catalyst, but due to the length of the project, it was decided to mainly focus on two ZSM-5 zeolites already available on site, namely [...] NH4-Z80 and NH4-Z23, both provided [...]. These two catalysts have a Si/Al ratio of [...] respectively, therefore different modification techniques are expected to be appropriate for each of the two.

For example, the NH4-Z80 catalyst possesses a Si/Al ratio that lies in the [...] range [...] determined by Groen et al. in which mesopores can be efficiently introduced by [...]. Furthermore, [...]. Therefore, this commercial catalyst was subjected to [...].

On the other hand, the NH4-Z23 catalyst has a Si/Al ratio [...]. As reported previously, a technique that allows for the formation of mesopores in ZSM-5 zeolites with Si/Al [...] is a [...]. These combined methods were therefore applied to the NH4-Z23 sample.

For completeness, the effect of the two procedures was tested on both catalysts. [...]

For a more detailed description of the modification procedures and the samples obtained in this project, the reader is referred to the methods (section 2.2).

2. Materials and methods

2.1. Chemicals and catalysts

The list of the chemicals specifications, including the catalysts, employed during this project is reported in Table 1.

Table 1: detailed list of chemicals employed.

Chemical	Trade-commercial name	Provider	Purity/composition	Other
Oleic acid	High Oleic Sunflower Oil HOSO (Priolene™ 6923)	Croda	81.4-81.7% $C_{18:1}$ 7.7-9.7% $C_{18:2}$ 0.8-1.0% $C_{18:3}$ 2.6-2.7% $C_{18:0}$	
ZSM-5 catalyst	[...]	[...]		Crystal size [...]
ZSM-5 catalyst	[...]	[...]	[...]	2–3 µm agglomerates made of ca. [...]
ZSM-5 catalyst	[...]	[...]	[...]	Average crystal size [...]
NaOH		J.T.Baker® BAKER ANALYZED A.C.S. Reagent	≥97%; Ca≤0.005%; Cl≤0.005%; K≤0.01%; Na_2CO_3<1.0%	pellets
HCl		J.T.Baker® BAKER INSTRA-ANALYZED™ Plus	w/w 34-37%; Br^-≤10ppm; P≤0.01ppm; S≤0.3ppm;	solution
NH_4NO_3		Merk KGaA, EMSURE® ACS	>95.0%	
Adam's catalyst (PtO_2)		Sigma Aldrich	Pt,80-85%	Surface area ≥75 $m^2 \cdot g^{-1}$
BF_3-methanol complex		Merk	20% solution in methanol	
Ethyl acetate		Croda	≤100%	

2.2. Catalyst modification

H-T22 is provided already in the H-form, which means that no activation is needed and the catalyst can be directly employed for the alkyl-isomerisation experiments as such. Furthermore, no modifications to introduce mesoporosity were applied to this catalyst, therefore the only sample of this catalyst used in this project is the commercial unmodified one, named H-T22 (H indicating the counteraction [...].

On the other hand, the two catalysts [...] were subjected to several modifications, with the intent of introducing mesopores. The steps involved in the preparation of these samples are reported schematically in Figure 18. The treatment **a** is used to activate the commercial NH_4-form samples to the acidic H-form, treatment **b** is the procedure to introduce mesopores by [...], while **c** is the [...]. Finally, **d** depicts the steps to [...]. The different steps of each procedure, i.e. [...] are often present in more than one procedure; therefore, to avoid repetitions, the single steps are here described in details separately, while the sequence in which they are used in each procedure can be deducted from Figure 18.

Figure 18: Schematic representation of the steps involved in the modification procedures of the zeolites to obtain a) activated H-form of the catalyst, i.e. a parent zeolite b) desilicated and activated H-form of the catalyst, c) dealuminated and activated H-form of the catalyst, d) desilicated and successively dealuminated activated H-form of the catalyst.

Calcination: Unlike the sample provided by [...], the two catalysts ex [...] are received in the NH_4-form. Therefore, a calcination step is required to activate them to the acidic H-form (Figure 18a). Specifically, 5 h at 500 °C are the conditions employed. This step was also applied at the end of each modification (Figure 18b-d), for the same reason.

[...] treatment: [...]

[...] wash: [...]

Ion exchange: As a consequence of the [...], therefore the zeolite needs to be exchanged back to the NH_4-form. For this reason, the catalyst was treated in 0.1 M NH_4NO_3 solution (10 g catalyst in 150 ml) for 4 cycles of 16 h, 7 h, 16 h and 7 h respectively. (Note that the difference in time among the 4 cycles was due to the day/night schedule).

Rinsing: After the [...] treatment, [...] or ion exchange steps the catalyst was rinsed consecutive times. Specifically, it was stirred in approximately 300 ml of distilled water for 45 minutes. The mixture was then centrifuged to remove the catalyst from the solution, and the pH of the solution checked. The catalyst was then rinsed again with fresh distilled water. This procedure was repeated until neutral pH was reached, generally up to 12-14 times.

Drying: Once the catalyst was treated and rinsed, a drying step was necessary before calcining the sample. Zeolites are generally very stable at high temperatures, but a too fast evaporation of the water contained in the particles of a wet sample might alter the zeolite. Therefore, the samples were generally dried on a heating plate set at 65 °C for 3 h and only then put in the oven for the calcination step. Furthermore, two extra steps (1 h at 85 °C and 5 h at 105 °C) were introduced in the oven program procedure, before the 5 h at 500 °C of the actual calcination.

To simplify the discussion, Table 2 reports a list of the samples names which are used when reporting the results and the corresponding treatment they were subjected to. The names were assigned this way: first, the counteraction of the sample is indicated (H or NH_4), then a letter indicating [...] and a number which refers to the [...]. Finally, a code for the treatment they were subjected to (AT and AW for [...]) to differentiate the several modified samples or P for the parent unmodified ones.

Due to practical reasons, the samples could not be synthesised in larger quantities. Therefore, every sample here considered was synthesised as part of a different batch. That is, when preparing the [...] treated catalyst with following [...] procedure, there was not enough of the [...] treated sample left and the preparation of the sample had to be started from a new lot of parent. Therefore, a direct comparison between [...] treated samples and those that also underwent a post [...] should be considered with caution.

Table 2: Samples name list, with corresponding information about the commercial name of the pre-treated sample and the specific treatment every sample was subjected to.

Sample name	Supplier, code, counteraction	Treatment*
H-T22	[...]	-
NH_4-Z23	[...]	-
NH_4-Z80	[...]	-
H-Z23-P	[...]	**a** (calcination)
H-Z23-AT	[...]	**b** [...]
H-Z23-AW	[...]	**c** [...]
H-Z23-AT+AW	[...]	**d** [...]
H-Z80-P	[...]	**a** (calcination)
H-Z80-AT	[...]	**b** [...]
H-Z80-AW	[...]	**c** [...]
H-Z80-AT+AW	[...]	**d** [...]

*The letters **a**, **b**, **c** and **d** refer to the scheme of Figure 18, where a more detailed picture of the treatments is provided.

2.3. Catalyst characterisation

In **nitrogen physical gas adsorption (N_2 physisorption)**, the cell holding the sample is evacuated and cooled to liquid nitrogen temperature (77 K); nitrogen gas is then dosed; it is partially adsorbed on the surface until reaching equilibrium with the bulk. Adsorbed nitrogen first forms a monolayer on the sample surface while further increase in pressure results in the formation of multilayers. At a given relative pressure (p/p_0), the amount of gas at a specific part of the surface of the solid sample depends on local surface-energetic properties and on the geometry of the surface itself. Adsorption and desorption points can be recorded at different pressures and isotherm curves can be constructed. In the region where monolayer and multilayers are formed, the specific surface area (S_{BET}) is determined according to the BET (Brunauer, Emmet and Teller) theory. This model is applicable to non-porous, meso- and macroporous materials and adsorption points in the p/p_0 range between 0.05 and 0.25 are typically used. However, for microporous materials, such as zeolites and activated carbon, the relative pressure range < 0.1 is recommended.

The **physisorption** investigations were performed on a Quantachrome Autosorb 6B adsorption analyser. Samples amount of 0.07-0.15 g (dried weight) were used for the analyses. The full adsorption and desorption isotherms with N_2 as adsorptive were recorded at 77 K in order to derive quantitative information on the specific surface area, pore size distribution and pore volume. Prior to these investigations, the samples were degassed at 350°C in vacuum for approximately 16 h.

In **ammonia temperature programmed desorption (NH_3-TPD)** studies, the acidity of the sample under investigation is measured by analysing the interaction of the NH_3 probe molecule with the surface of the solid sample as a function of temperature. The basic NH_3 probe molecule can interact with Lewis and Brønsted-type acid sites, which depending on the interaction release the NH_3 molecules at lower (weak acid sites) or higher (stronger acid sites) temperature. The temperature at which NH_3 is released

provides qualitative information on the acid strength whereas the amount of NH_3 desorbed provides quantitative information on the total acidity of the sample.

The NH_3-TPD investigations were performed on a Micromeritics TPD/TPR 2900 analyser. A TPD curve ranging from 473 K up to 823 K has been recorded to quantify and qualify the acidic properties of the samples. The sample was held in a quartz reactor and placed into the Micromeritics TPD/TPR 2900 analyser for in-situ pre-treatment and successive NH_3-TPD analysis. In the TPD analyser, the sample was subjected to a temperature program from room temperature up to 823 K (550 ºC) in helium, using a ramp rate of 10 $K \cdot min^{-1}$. The sample was kept at 823 K for 30 min in flowing helium. Then, after cooling down in helium to 473 K (200 ºC), the sample was alternately flushed with ammonia for 10 min and with helium for 10 min. This procedure was repeated 3 times. After the third flushing step, the conditions were held constant until a stable baseline was obtained. Finally, desorption of ammonia was monitored in the temperature range of 473-823 K (ramp rate 10 $K \cdot min^{-1}$).

Both N_2 physisorption analyses and NH_3-TPD were performed externally by Delft Solid Solutions.

Thermo-Gravimetric Analyses (TGA) of the catalysts were performed on a Mettler Toledo TGA/DSC3+. For all analyses, 10 mg of the sample (±0.2 mg) were placed in an aluminium crucible. The measurements were carried under air flow rate of 60 ml/min and heating rate 15 ºC/min, from RT to 600 ºC.

2.4. Catalytic testing

The **alkyl-isomerisation reactions** to test catalyst performances were conducted in a mini-PARR® autoclave (Series 5500 High Pressure Compact) combined with a 4848 Reactor Controller (both from Parr Instrument Company). All reactions were carried out with 25 g Oleic Acid (Priolene™ 6923), 0.15 g distilled water and [..]g catalyst for [..] % reactions, or [..]g catalyst for reactions at [..] % loading (the catalyst loading of each reaction is always specified when reporting the results). After purging with nitrogen 3 times, the reactor was pressurised to about 1 bar and heated to 260 ºC, under mechanical stirring (650-700 rpm), resulting in a pressure of 4-6 bar. Due to the small capacity of the reactor, only one sample could be taken during the course of the reaction without disturbing the reaction conditions. A second sample was then obtained at the end of the reaction, after cooling down of the reaction mixture. Therefore, in order to be able to obtain a conversion curve with 4 points, 2 experiments were conducted for each catalyst sample. Once the sample of the product mixture was cooled down to temperatures below 80 ºC, it was filtrated from the catalyst with a 0.45 μm PTFE membrane filter (MicroSolv AQ™), then analysed.

Some of the samples were also tested with a second reactor, specifically a 1.8 L RC1 high-pressure reactor from Mettler Toledo. 800g of the OA feed, with [..] of catalyst ([..]% loading) and 5 g demineralised water. The reactor was first purged 3 times with nitrogen, pressurised to about 1 bar and heated up to 260 ºC, while increased to 8 bar. The reaction mixture was stirred at 400 rpm. For the experiments with this reaction, longer reaction times were possible and multiple samples could be taken from a single experiment. However, only the H-T22 catalyst and the parent H-Z80-P and H-Z23-P were available in sufficient quantity to be tested in this reactor.

During the experiments, two different batches of the oleic acid feed were employed (both coming from the same Priolene™ 6923). The two batches were therefore analysed and the composition was verified to vary slightly, mainly in the content of linoleic acid ($C_{18:2}$) (see feed composition ranges reported in Table 1). Nonetheless, the effect on the overall conversion and on the product composition was verified to be of a very limited importance.

The **composition of the product** mixtures samples obtained by alkyl-isomerisation were tested in two ways, as depicted in the scheme reported in Figure 19. First, **the monomer and oligomer content** of the mixture was determined by High-Temperature Gas

Chromatography (**HTGC**), after **methylation** of the sample with BF_3-methanol. The GC (Agilent 7890) was equipped with a cold on-column injection and a metal column with a non-polar stationary phase Cp-SimDist Ultimetal (Chromopack WCOT, 5 m x 0.53 mm x 0.17 μm). A Flame Ionisation Detector (FID) was used for the detection of the components. The injection volume was 1μl for a concentration of 20mg/ml in heptane and the injection temperature 50 °C. The carrier gas was nitrogen with a constant flow of 10 ml/min and a column pressure of 20kPa (3Psi). The temperature program was as follows: initial temperature of 60 °C (held for 1 min), temperature increased to 150 °C with 30 °C/min ramp (held for 0 min), temperature increased to 375 °C with a 12 °C/min ramp (held for 5 min). The FID detector temperature was set a 375 °C.

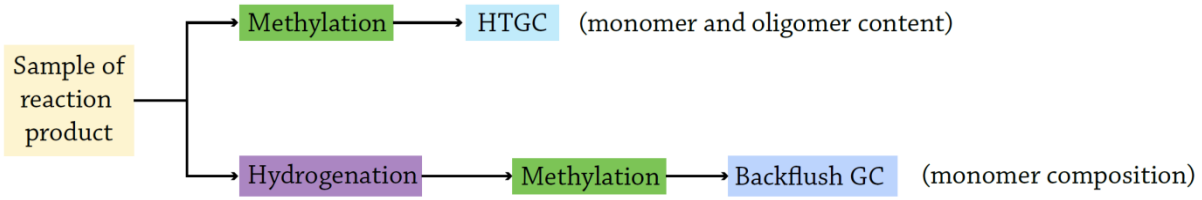

Figure 19: Schematic representation of the analysis steps to determine the monomer and oligomer content of the alkyl-isomerisation reaction samples (top) and the specific monomer composition of such samples (bottom).

Secondly, to obtain the **monomer composition**, the sample was hydrogenated, methylated and analysed by **backflush GC**. Back-flushing works by reversing the column flow immediately after the last compound of interest has eluted, thereby sweeping material backwards through the column and out the split vent, allowing saving a substantial amount of time for each analysis. In fact, only the monomer composition is of interest for the purpose of this project. Specifically, the content of mono- and poly-branched C_{18} fatty acids, as well as the amount of unreacted C_{18} species is significant for the determination of the catalyst performance. Since the oligomer fraction is "back-flushed" from the column, this technique allows to run a GC analysis and to determine the monomer composition, without prior separation of the monomer from the oligomer.

The **hydrogenation** of the sample was performed before methylation and backflush GC to reduce the complexity of the samples and facilitate analyses. Specifically, by diluting in ethyl acetate to a 40 mg/ml concentration, and using 20 mg of Adam's catalyst, reduced in situ at RT with a hydrogen flow of 50 ml/min, for 10 minutes. The following **methylation** was also in this case performed with BF_3/methanol. The so-obtained hydrogenated and methylated sample was then subjected to backflush GC. The GC was equipped with a split injection and a fused silica retention gap column with a polar stationary phase CP-FFAP-CB (25 m x 0.32 mm x 0.30 μm). The sample volume injected was 1 μl for a concentration of 10 mg/ml in heptane. The carrier gas was hydrogen and the temperature program as follows: initial temperature at 50°C (held for 1 min), then increased to 250°C with a 10°C/min ramp (held for 4 min).

The reactive components of the feed are considered to be the oleic acid ($C_{18:1}$), linoleic acid ($C_{18:2}$) and linolenic acid ($C_{18:2}$). The conversion of these unsaturated components was calculated with the following formula:

$$conversion = y_t = 1 - \frac{[(x_{C18,t}+x_{C18:1,t})\times y_{M,t}-x_{C18,0}]}{[x_{C18:1,0}+x_{C18:2,0}+x_{C18:3,0}]} \qquad \text{Eq.1.1}$$

The onset of the reaction (t=0) was set at the time when the reaction mixture reaches the designated 260 °C. Therefore, [$x_{C18:1,0}$ + $x_{C18:2,0}$ + $x_{C18:3,0}$] is the sum of the initial mass fractions of oleic, linoleic and linolenic acid in the feed. The mass fraction of the stearic acid in the hydrogenated monomer as a function of time is indicated as $x_{C18,t}$, and summed to the mass fraction of oleic acids $x_{C18:1,t}$ still found after hydrogenation, gives a quantitative indication of the reactant that did not undergo conversion. To obtain an accurate conversion, such sum must be normalised considering the monomer content of the sample ($y_{M,t}$) revealed by HTGC analysis, and subtracting the initial mass fraction of stearic acid already present in the feed ($x_{C18,0}$), also determined by HTGC.

A detailed identification of the species found in the product is out of the scope of this project. However, it is important to verify that the zeolites tested give products made of similar components. In Figure 20, a section of the chromatogram patterns of the product mixture obtained by three different catalysts is reported. Although the distribution of the peak areas is specific to each chromatogram, the peak positions are matching and no extra peak is present in any of the chromatogram displayed. The same can be said for the complete chromatogram of all the samples tested, although not here reported. Therefore, all products synthesised using the modified and unmodified catalysts contain similar species, albeit in different proportions.

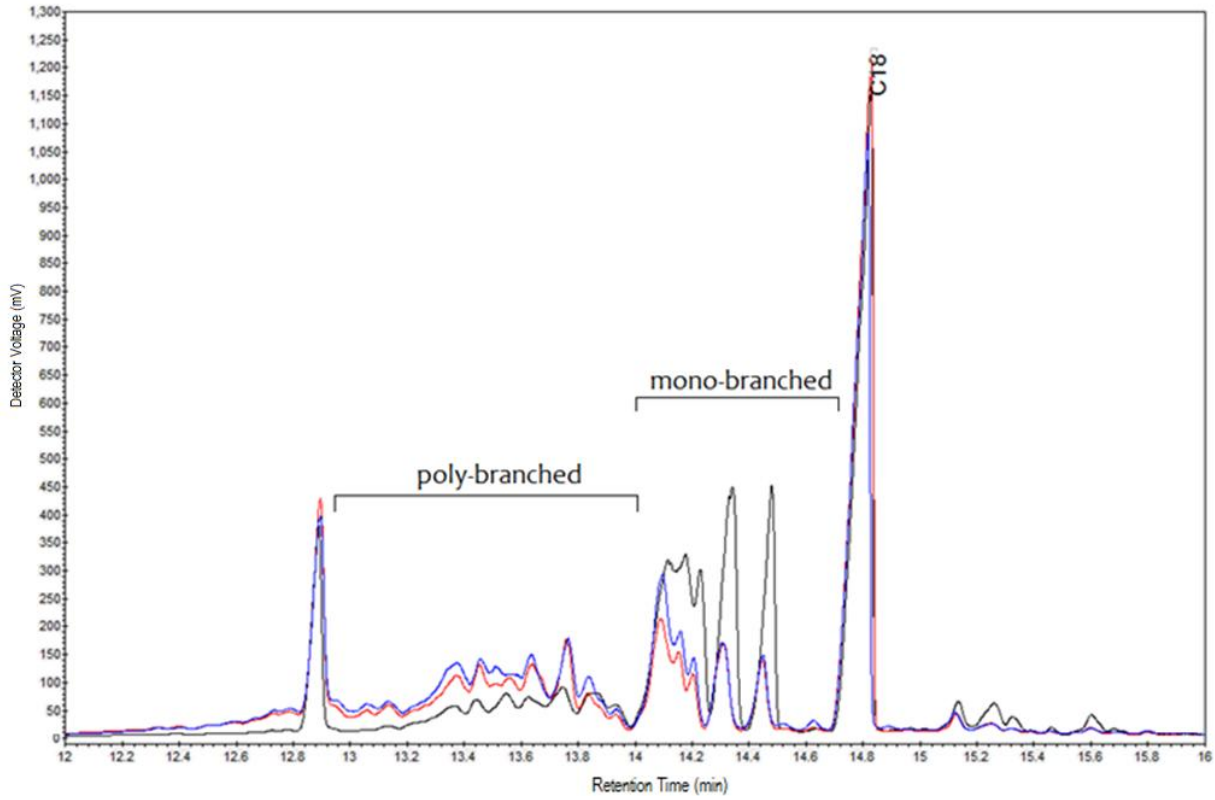

Figure 20: GC chromatogram of the C_{18} species elution time. The brackets indicate the regions of the poly-branched and mono-branched C_{18} peaks. Three chromatograms are reported for three alkyl-isomerisation samples using three different catalysts, at approximately the same oleic acid conversion (~60%): H-T22 (red), H-Z80-AT (blue) and H-Z23 (black). Although only these samples are here compared, all the other modified and unmodified catalysts gave product mixtures with similar GC chromatograms.

Because the relative content of mono-branched and poly-branched FA is determinant for the final product quality, it is important to verify the branching patterns of the different samples. The ratio between poly-branched and mono-branched FA was calculated as:

$$\frac{polybranched}{(polybranched+monobranched)} = \frac{polybranched}{x_{B,t}} \qquad \text{Eq.1.2}$$

This value is useful when comparing the branching pattern of the different samples. In fact, a desirable catalyst should not only give high conversions and high branching yield, but also give a product with an appropriate ratio between poly- and mono-branched FA, to better match the ISAC composition.

3. Results

3.1. Catalysts characterisation

Due to limited resources, only a few catalysts were characterised by N_2 physisorption and NH_3-TPD, namely the H-T22 reference, H-Z23-P, H-Z23-AT+AW and H-Z80-AT samples. The characterisation of the catalyst currently considered as the best performing material, H-T22, was considered as essential; to the best of our knowledge, this is the catalyst with the highest performance identified to date and the scope of the project is to find improvements. Therefore, having a better insight into what differentiate this catalyst from other ZSM-5 is of primary importance. Furthermore, characterisation of the parent zeolites would also allow a better understanding of the effect of the modification techniques applied to the two commercial catalysts. However, the NH_4-Z80 commercial catalyst has been widely described in literature and the method used for its calcination to the H-form is the same as that employed during this project. Therefore, for this specific sample it was considered reliable to use the data found in literature. On the contrary, data found on the NH_4-Z23 catalyst were insufficient; therefore, the H-Z23-P sample was also characterised. As for the treated sample, one for each catalyst was chosen, specifically those with the best improvement from the parent zeolite, namely H-Z80-AT and H-Z23-AT+AW.

3.1.1. N_2 Physisorption

Adsorption and desorption isotherms are depicted in Figure 21. The Figure shows that the isotherms of samples H-T22, H-Z23-P and H-T23-AT+AW show predominant uptake at lower relative pressures, indicating a high level of microporosity. At higher relative pressures only a minor increase in uptake can be seen for H-Z23-P, suggesting that this sample does not contain mesoporosity. However, a slightly higher increase in uptake is shown at high relative pressure for H-T22 and H-T23-AT+AW, which might indicate a minor level of mesoporosity. On the other hand, the isotherm of sample H-Z80-AT shows a substantial uptake at lower relative pressures, corresponding to a high level of microporosity, yet this sample also has a large uptake at higher p/p_0 values and displays a hysteresis loop; therefore, substantial mesoporosity should be present. The textural composition values derived from the isotherms are reported in Table 3.

The specific surface areas of the samples are in the range between 337 - 543 $m^2 \cdot g^{-1}$. Coupled to the sample weights used in the investigations, the measured absolute surface areas are adequate to obtain fully accurate results. Under these conditions, the error is estimated at < 3% relatively. It can therefore be concluded that the specific surface areas of samples H-T23-P and the modified H-Z23-AT+AW are not significantly different compared to each other (371 and 384 $m^2 \cdot g^{-1}$, respectively), that the surface area of sample H-T22 is significantly the lowest (337 $m^2 \cdot g^{-1}$) and that sample H-Z80-AT has the highest specific surface area (543 $m^2 \cdot g^{-1}$). If we consider the data on H-Z80-P obtained from literature, we can conclude that the [...] treatment induced an enhancement of surface area on the H-Z80 catalyst.

The micropore volumes (V_{micro}) of the samples are the major contributor to the specific surface area and are rather similar compared to each other, as they are in the range between 0.114 – 0.139 $cm^3 \cdot g^{-1}$. The micropore volumes of samples H-T23-P and H-Z23-AT+AW are very similar and that of sample H-T22 is somewhat lower, but similar to the micropore volume of sample H-Z80-AT.

Table 3: Textural composition of the ZSM-5 samples derived from the adsorption isotherms.

Sample	S_{BET} [a] ($m^2 \cdot g^{-1}$)	S_{meso} [b] ($m^2 \cdot g^{-1}$)	V_{pore} [c] ($cm^3 \cdot g^{-1}$)	V_{micro} [b] ($cm^3 \cdot g^{-1}$)	$V_{meso}+V_{macro}$ ($cm^3 \cdot g^{-1}$)
H-T22	337	40	0.323	0.119	0.204
*H-Z80-P**	*[…]*	*[…]*	*[…]*	*[…]*	*[…]*
H-Z80-AT	543	268	0.926	0.114	0.812
H-Z23-P	371	29	0.201	0.139	0.062
H-Z23-AT+AW	384	61	0.259	0.134	0.125

(a) BET method; (b) t-plot method; (c) Volume adsorbed at p/p_0=0.99; *data from literature[8,14,49,52]

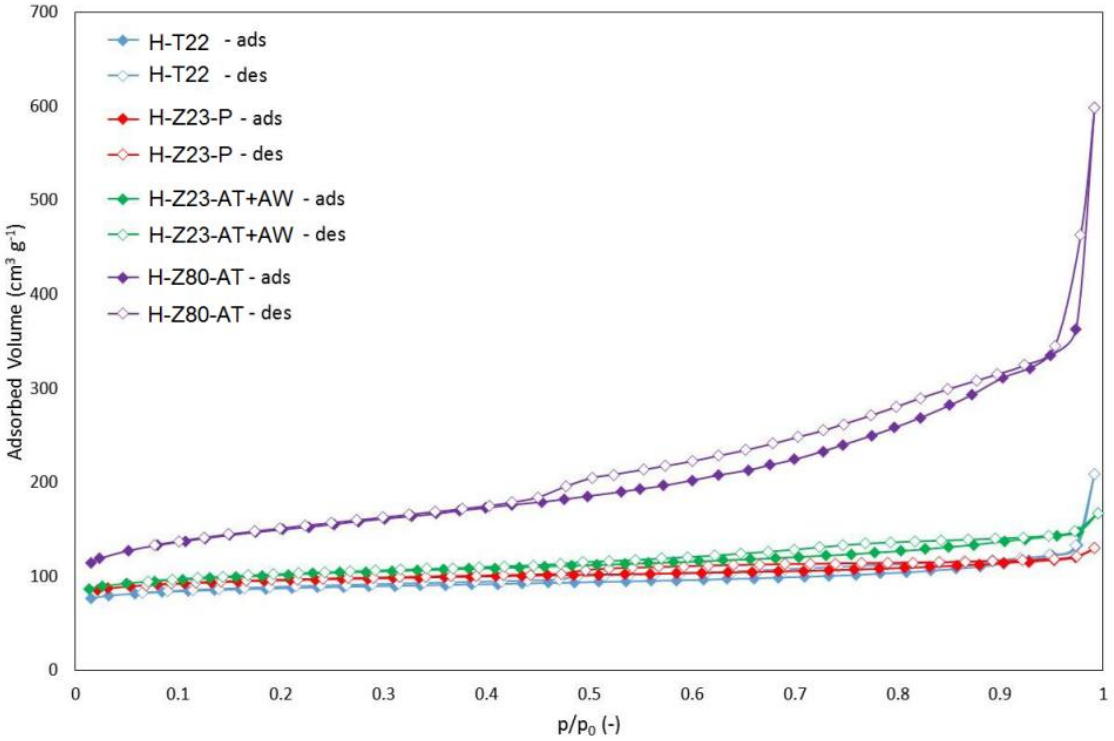

Figure 21: N_2 adsorption and desorption isotherms at 77 K of the four ZSM-5 samples. Closed symbols denote adsorption, open symbols denote desorption. (Provided by Delft Solid Solutions).

The pore size distributions of the samples are displayed in Figure 22. It can be seen that the curve of the untreated H-T23-P sample shows no significant peaks in the mesopores range (2-50 nm). In the case of samples H-T22 and H-Z23-AT+AW, the pore size distributions are very similar, showing a marginal mesoporosity in the range from 2-50 nm. This supports that the modification on H-Z23 with [...] treatment and successive [...] introduced minimal mesoporosity, probably only modifying the external side of the catalyst. However, sample H-T22 shows also some macroporosity (> 50 nm), which leads to the higher total pore volume of this sample, as seen in Table 3. Unlike the other catalysts tested, the [...] treated H-Z80-AT does show distinct mesoporosity ranging from 2 to 50 nm, with a mode around 8 nm. Furthermore, the sample also displays some macroporosity.

For all four samples, the fact that the distributions have not returned to baseline level around 2 nm is again an indication of the presence of micropores.

As a further confirmation of the successful introduction of mesopores in sample H-Z80-AT, we can compare the results to those reported in the literature for the commercial H-Z80-P (also reported in Table 3). We can conclude that the [...] treatment on H-Z80 has led to a high degree of mesoporosity (S_{meso} from 45 $m^2 \cdot g^{-1}$ to 268 $m^2 \cdot g^{-1}$), enhancing the specific surface area, while limitedly

impacting the intrinsic micropore volume (0.160 $cm^3 \cdot g^{-1}$ to 0.114 $cm^3 \cdot g^{-1}$). The surface area of the parent zeolite is already relatively high, probably due to the high microporosity and relatively small sized crystals ([…] reported average).[52]

On the other hand, the modification treatment on H-Z23 has only limitedly induced new mesoporosity (S_{meso} from 29 $m^2 \cdot g^{-1}$ to 61 $m^2 \cdot g^{-1}$), most likely only affecting the external surface of the catalyst.

As for the H-T22 sample, which was purchased as such and not modified, mesoporosity seems to be present at a very marginal level, while macropores are present to a higher extent. Since the crystals of this catalyst are reported to be of an average size of […], the relatively low surface area could be ascribed to the low microporosity, which is, in general, the major contributor to S_{BET}. Furthermore, the macropores (and mesopores) could arise from the presence of voids between such small sized crystals when closely packed together. The presence of macropores in H-Z80-AT could be also ascribed to this phenomenon, as the crystal size of its parent zeolite is also reported to be relatively small, although bigger than the H-T22 sample. Furthermore, [...] treatment in the H-Z80-AT sample might also have contributed to its macroporosity.

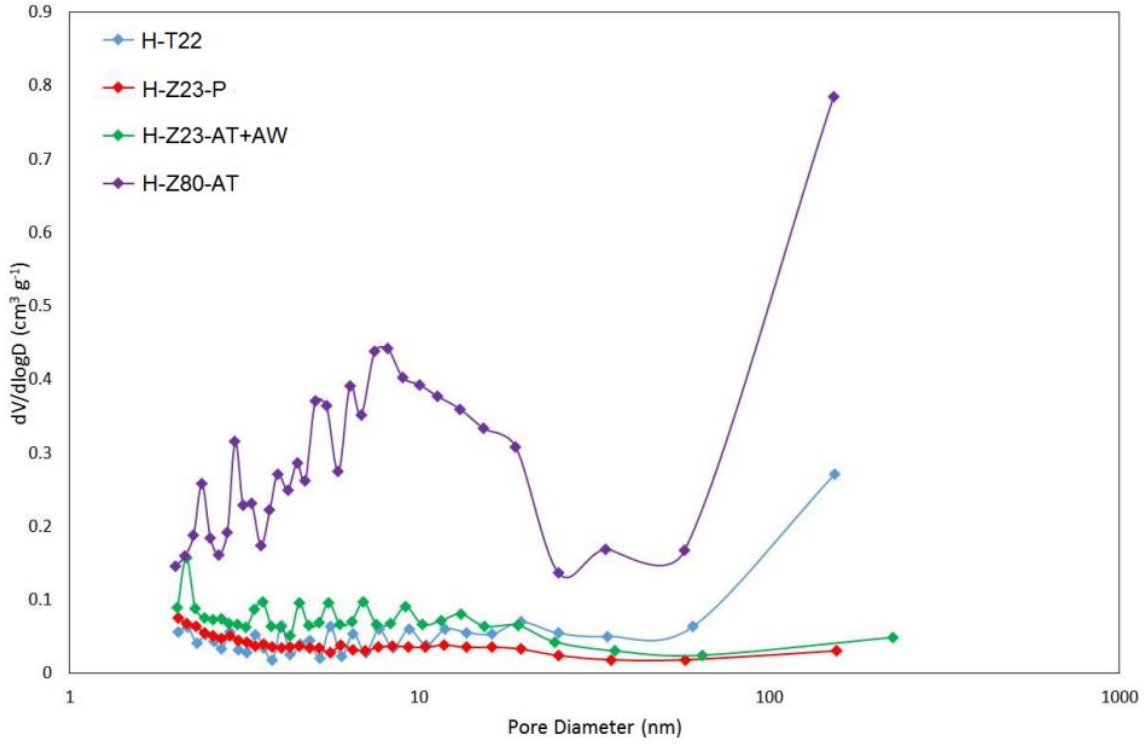

Figure 22: BJH pore size distributions of the four ZSM-5 samples derived from the adsorption branch of the isotherms in Figure 21. (Provided by Delft Solid Solutions).

3.1.2. NH_3-TPD

For each NH_3-TPD analysis, between 0.07-0.13 grams of sample were used in order to have the most representative sampling. The dry sample weight, obtained by weighing the sample after the analysis, has been used in the calculations. The quantitative results of the samples are displayed in Table 4. The total NH_3 uptake has been calculated via integration of the desorption profiles depicted in Figure 23; the area underneath the curve is determined and corresponds to the total amount of NH_3 that is desorbing from the sample. As the temperature becomes stable, the signal rapidly drops towards the baseline. This is due to the fact that the NH_3 concentration that is desorbed by the sample also rapidly decreases, but also indicates that at the maximum applied temperature of 823 K some desorption still occurs. The relative standard deviation, determined over an in-house standard, is approximately 7% for NH_3-TPD investigations.

Table 4: Acidic characteristic of modified and unmodified ZSM-5 samples, tested by NH_3-TPD analysis.

Sample	Weight loss (%)	Si/Al*	Total NH_3 uptake (mmol•g^{-1})
H-T22	14.1	11	1.248
H-Z80-AT	12.1	<40	0.366
H-Z23-P	12.7	11.5	1.141
H-Z23-AT+AW	8.9	-	0.433

*For the parent catalysts, Si/Al was estimated from the SAR (SiO_2/Al_2O_3) provided by the manufacturer. For the H-Z80-AT, assuming Si was selectively removed from the framework, it is expected that the obtained catalyst would have Si/Al lower than its parent. No sufficient information were obtained for the H-Z23-AT+AW to know if more Si or Al were removed upon modification, therefore the Si/Al range is not reported.

In the NH_3-TPD curves, peaks are observed in two temperature regions, below and above 650 K, referred to as low-temperature (LT) and high-temperature (HT) region, respectively. The peaks in the HT region are generally assigned to desorption of NH_3 from strong Brønsted and Lewis sites, while the assignment of the peaks in the LT region is somewhat controversial in literature. For example, early articles report the concentration of the OH-groups calculated by IR spectroscopy to be proportional to the peaks area of both HT and LT regions, which suggested that the LT peak was also connected to the strongly acidic hydroxyl sites.[64] However, the LT peak could also be ascribed to the presence of weaker silanol (Si-OH) groups on the external surface or 'non-zeolitic' impurities.[65] Later studies suggested instead that extra-framework aluminium species with weak Lewis acidity could be responsible for the LT desorption peak of NH_3.[10,66] Finally, it was also proposed that the formation of ammonia H-bonded associations $[NH_4^{\bullet}nNH_3]^+$ could also take place during NH_3-TPD analyses. These protonated ammonia associations could release NH_3 and contribute to the LT peak.[67,68] Therefore, care must be taken when assigning the TPD peaks to specific species that could be present in the zeolites. In order to be able to identify the different acidic species of the catalyst samples, further analyses should be undertaken, such as FTIR analyses with probe molecules like pyridine.

Nonetheless, the TPD profiles can be useful to compare different zeolites and the total NH_3 uptake can give an indication of the acidity of the analysed samples. For the catalysts tested, Figure 23 shows that most of the profiles display a different trend. The curve of sample H-T22 shows initial desorption of NH_3 in the LT region, corresponding to weaker acidic sites (possibly Lewis sites associated with extra-framework Al species). After this initial desorption, a second peak can be discerned in the HT region, with a maximum around 680 K and a shoulder at higher temperatures. This second peak corresponds to stronger acidity, which is likely linked to Brønsted acid sites, as expected by the low Si/Al ratio of the catalyst. The total NH_3 uptake is the highest of the tested samples (1.248 mmol•g^{-1}).

The profiles of samples H-Z23-P and the modified H-Z23-AT+AW display a similar trend, albeit at a lower intensity for sample H-Z23-AT+AW. This indicates that upon the modification treatment of sample H-Z23-P resulting in sample H-Z23-AT+AW, not much extra mesoporosity is generated (see physisorption analyses) but a substantial loss in acidity is recorded (from 1.141 to 0.433 mmol•g^{-1}). Again, some initial desorption can be seen in the LT region, with a maximum slightly shifted to higher temperatures for the H-Z23-P than for the H-Z23-AT+AW sample. A second broad desorption signal in the HT region is also present, although both H-Z23 samples do not show the substantial contribution of acidic sites around 680 K, that sample H-T22 does show.

Sample H-Z80-AT displays a gradual NH_3 desorption increase up to 680 K where a maximum is reached, after which a steady decrease can be observed. Hence, if the peak at LT regions is in fact due to EFAl, the H-Z80-AT sample seems to not have a significant amount of these species, while most of the acidic sites of this sample are anticipated to be strong Brønsted ones. However, the total NH_3 uptake is the lowest among the tested samples and corresponds to 0.366 mmol•g^{-1}. This could be due both to the effect of the modification procedure, but also to the expected low acidity of the parent zeolite, ascribed to the high Si/Al ratio, i.e. low Al concentration.

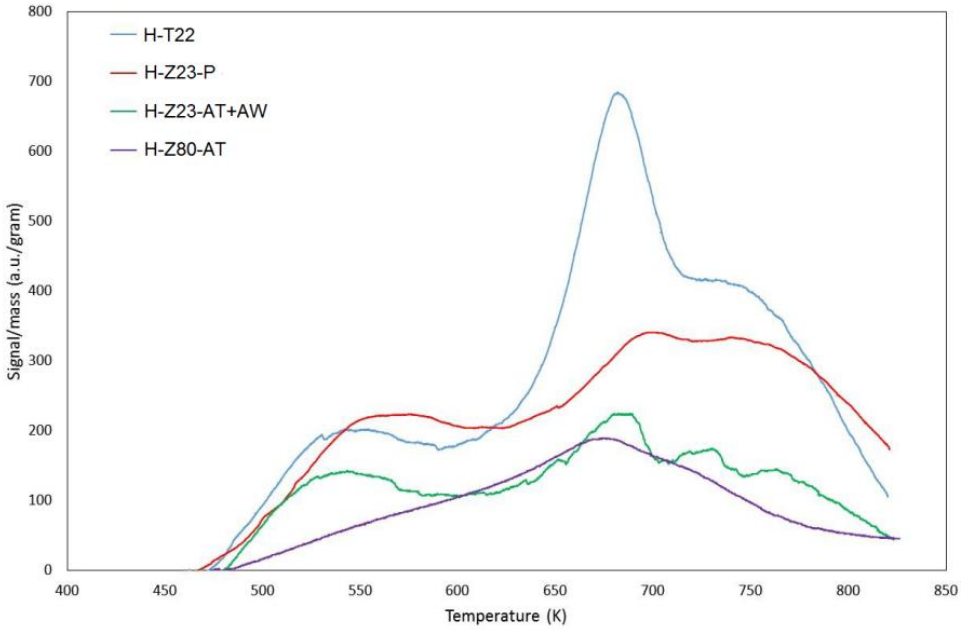

Figure 23: NH_3-TPD profiles for the four ZSM-5 samples tested. (Provided by Delft Solid Solutions).

3.1.3. TGA

TGA is not a technique commonly used for the analyses of the zeolite catalysts properties, since quantitative information related to textural structure or acidity of a sample cannot be directly derived. However, it can still be employed for a qualitative investigation of the effects generated by the modifications applied on commercial catalysts. Zeolites are expected to be stable at temperatures up to 500 ºC. Furthermore, when the tested samples are in the H-form, the weight loss upon thermal treatment is expected to be mainly due to water release. Zeolites with different acidity bond to water more or less strongly. Furthermore, the textural properties of the catalysts, i.e. the type of porosity, should allow for different quantities of water to be absorbed into the catalyst particles. Hence, as an available technique on site, TGA was used as a qualitative method to verify the effect of the different modification procedures on the ZSM-5 catalysts.

Figure 24 shows the TGA profile and the first derivative of such curve for the H-Z80 parent and derived samples. It is clear that the parent and the [...] zeolite have very similar weight loss profiles, while the samples that underwent [...] treatment, followed or not by [...], have a greater total weight loss compared to that of the parent (9% against 6%). The presence of multiple peaks in the derivative curve (i.e. different inflexion point in the weight loss curve, indicating different speed of loss) shows that the weight loss occurs in different steps. The different steps of weight loss are reported in Table 5, together with the total % weight loss. In all cases, most of the weight is lost while reaching temperatures of 100 ºC, suggesting that the loss is indeed due to weakly bonded water release.

The TGA profile and the first derivative curves of the H-Z23 parent and treated samples are very similar to each other and to that of the H-T22 catalyst, as seen in Figure 25. However, they all have a greater weight loss percentage than the H-Z80 samples (9,5-12% against 6-9%). This could be due to the general higher acidity of the samples with lower Si/Al ratio (H-Z23 and H-T22). In fact, the H-Z23 sample with lowest weight loss percentage is the H-Z23-AT+AW. This sample has a total weight loss of 9.33 %, which is very close to the H-Z80-AT (8.99%). While both H-T22 and H-Z23 revealed high acidity by NH_3 uptake, the treatment of the H-Z23 with [...] solution and following [...] showed to reduce significantly the NH_3 uptake (lowering it from 1.141 to 0.433 $mmol \cdot g^{-1}$, see Table 4) bringing it almost to the level of NH_3 uptake of the H-Z80-AT. On the other hand, desilication of the H-Z80 sample should lower the Si/Al ratio of the zeolite, and this could be the cause of the increased weight loss in the H-Z80-AT sample

compared to the parent. However, from physisorption data, the presence of mesopores in this [...] treated sample was also confirmed. This might also allow for a higher content of water in the zeolite and, therefore, a bigger weight loss % when submitted to thermogravimetric analyses.

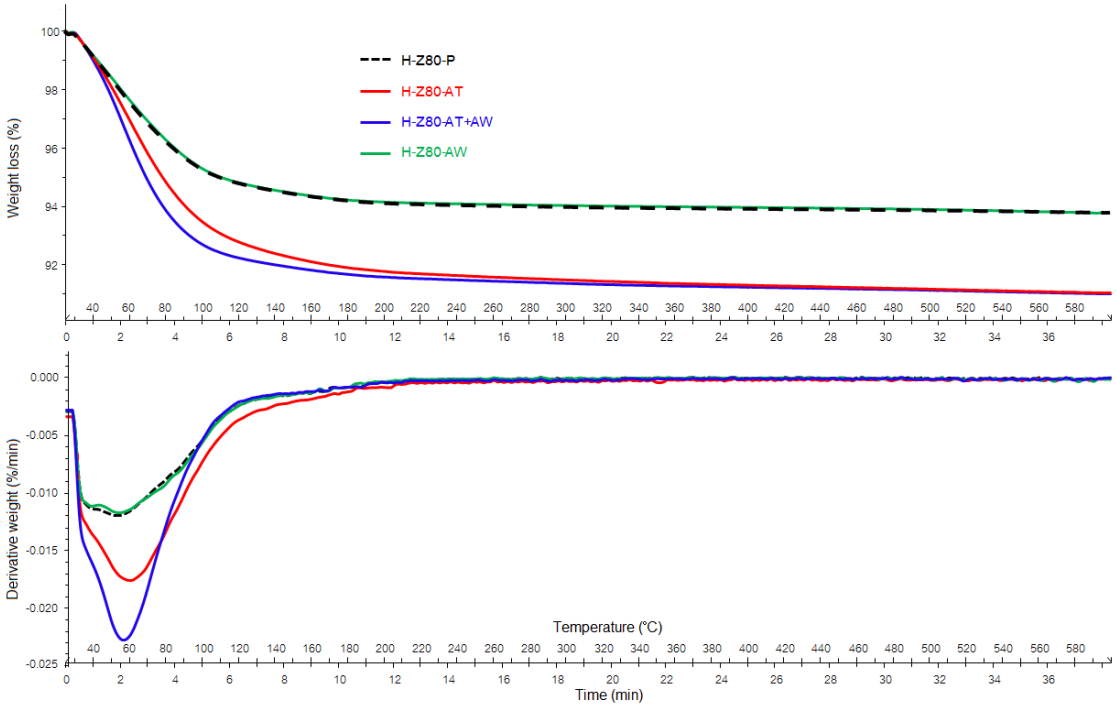

Figure 24: TGA profiles (top) and first derivative (bottom) of the four ZSM-5, modified and parent H-Z80 samples.

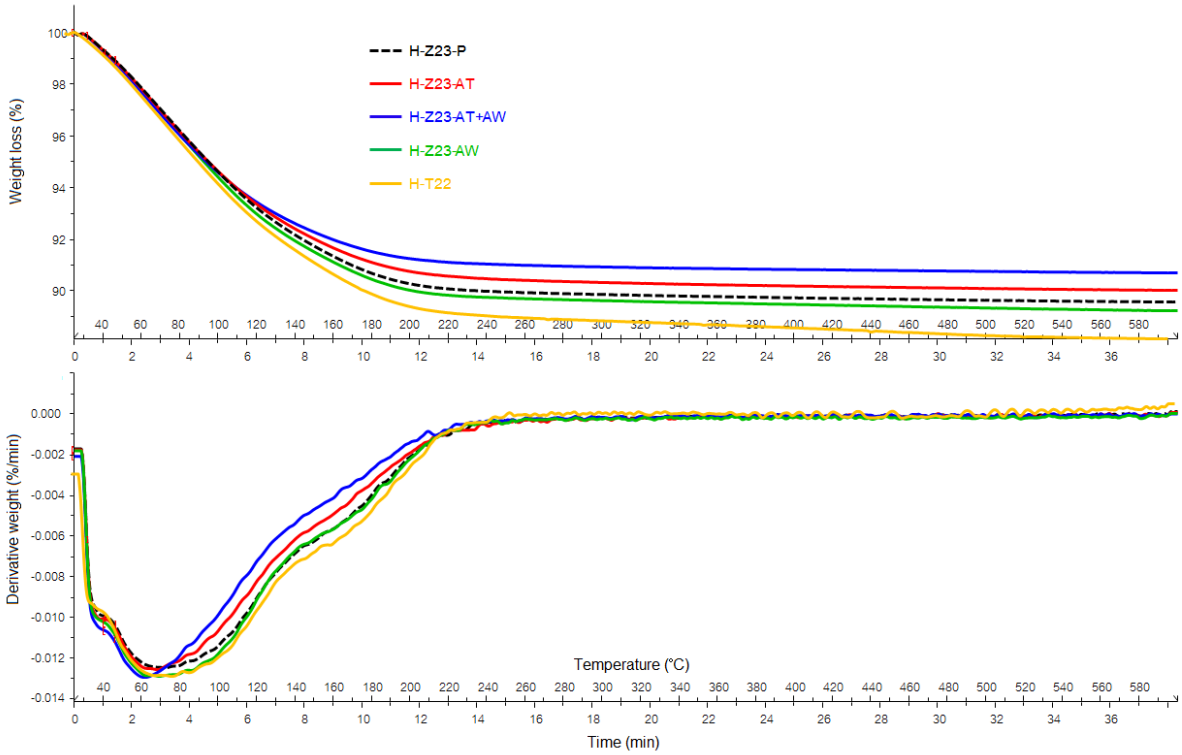

Figure 25: TGA profiles (top) and first derivative (bottom) of the modified and parent H-Z23 samples and the H-T22.

Table 5: Weight loss and steps of the ZSM-5 samples analysed, derived from the TGA profiles of Figure 24 and Figure 25.

Sample	% Weight loss per step			
	Step 1 (~ 25-140 ºC)	Step 2 (~140-260 ºC)	Step 3 (~260 - 600 ºC)	Total
H-T22	8.05	2.99	0.77	11.80
H-Z80-P	5.37	0.55	0.28	6.19
H-Z80-AT	7.47	0.85	0.67	8.99
H-Z80-AT+AW	8.47	-	0.53	9.01
H-Z80-AW	5.39	0.53	0.36	6.27
H-Z23-P	7.94	2.12	0.37	10.44
H-Z23-AT	7.53	2.05	0.39	9.97
H-Z23-AT+AW	7.53	1.49	0.32	9.33
H-Z23-AW	8.12	2.20	0.47	10.78

3.2. Catalyst testing

In order to confirm the hypothesis that mesoporosity introduction in ZSM-5 zeolites should increase catalyst's activity for the alkyl-isomerisation of OA, all the prepared samples were tested in a mini-PARR reactor, including the untreated ones (parent catalysts) and the H-T22 catalyst, hence considered the reference to outperform. This way, the effect that the treatments have on catalyst performance can be verified and, in the case of a catalyst with good activity, a direct comparison with the H-T22 can be made.

Because the recently acquired mini-PARR reactor could not be left running overnight, only experiments up to 8h could be conducted. Therefore, to ensure that almost complete conversion would be reached, the first tests were run at a [..] % catalyst loading. However, one of the modified H-Z80 samples was obtained in too small amounts to allow testing at [..]% loading, namely the H-Z80 subjected to [...] treatment and consecutive [...] (H-Z80-AT+AW). Furthermore, the reference H-T22 loading was set at [..]; hence, further tests of alkyl isomerisation were also performed at such loading.

The results are here presented for the H-Z80 and H-Z23 separately.

3.2.1. H-Z80, [..]% loading

The unmodified H-Z80 (H-Z80-P) is expected to have a low activity compared to the H-T22 sample, due to their different Si/Al ratio and, therefore, different concentration of Brønsted acid sites. As shown in Figure 26, after a reaction time of 5.5 h, the oleic acid conversion characterising the H-T22 catalyst is already 94%, while it only reaches 56% with H-Z80-P. The [...] treatment on H-Z80 seems to have a positive effect on the catalyst performance, but a real significant improvement is obtained by subjecting the catalyst to [...] treatment. In fact, very similar conversions are obtained with H-Z80-AT and H-T22 (~95% conversion after 5.5-6h reaction time). From the physisorption data, it is known that the [...] treatment was successful in the introduction of mesopores in the H-Z80 catalyst. Hence, the beneficial effect from the presence of mesopores, in improving the accessibility to the active sites of the catalyst, is clearly shown by the higher conversion of the mesoporous H-Z80-AT sample, when compared to its microporous parent.

[Confidential]

Figure 26: Conversion vs reaction time of the unmodified and modified H-Z80 samples, compared to the current best material, H-T22. The [...] treated sample (H-Z80-AT, in red) shows a significant improvement from the parent, to the point of reaching the conversion obtained by the H-T22 sample. All the experiments were carried out with a catalyst weight loading of [..] and 25 g of feed in a mini-PARR autoclave.

In order to find a catalyst with a desirable performance, not only its activity should be high (high conversion in shorter times), but the branched FA compositions should be close to that of the product obtained by H-T22 reference catalyst. Since all catalysts tested are of the same zeolite type, ZSM-5, it is expected that they result in products made of similar species. A complete analysis of the product composition being out of the scope of this project, a general comparison of the chromatograms obtained by GC analyses has been done. As expected, when comparing the chromatograms of samples obtained by H-T22, H-Z80-P and H-Z80-AT catalysis, new peaks are not found. The only difference observed in the three chromatograms is the relative intensities of the peaks, which indicates that the different branched monomers are present in different relative quantities, depending on the specific catalyst employed in the reaction (see Methods section 2.4). Therefore, to check if a catalyst could be a valid substitute to the H-T22, the relative quantities of the resulting branched FA should be very similar.

For this scope, the ratio between poly-branched FA percentage and the total amount of branched FA (which includes both poly-branched and mono-branched FA) is calculated for every product's sample, and used as a good indication of the branching pattern of the samples. This value gives an indication of the proportion between the selectivity toward mono-branching and that toward poly-branching and it is sufficient to compare the selectivity of the different catalysts. The poly/(poly+mono) ratio values for the products obtained by the tested catalysts are represented in Figure 27.

It is evident that the products obtained with the H-T22 catalysts have higher poly-branched FA content, when compared to the unmodified H-Z80-P or the [...] H-Z80-AW. On the other hand, the [...] treated sample, which also shows high activities, gives a product with similar branching pattern to that of the H-T22.

However, it seems like the poly/(poly+mono) ratio is following an exponential trend, but that the products obtained by H-T22 and H-Z80-AT at lower conversion do not follow this trend. The mismatch is even more evident when the poly-branched yield and the mono-branched yield are represented in separate graphs, as in Figure 28, rather than a ratio value. Specifically, if we consider conversion around 80%, the poly-branched yield seems to be higher than what would be expected, while the mono-branched yield is lower. A possible explanation for this behaviour is given in the discussion (see section 4.4).

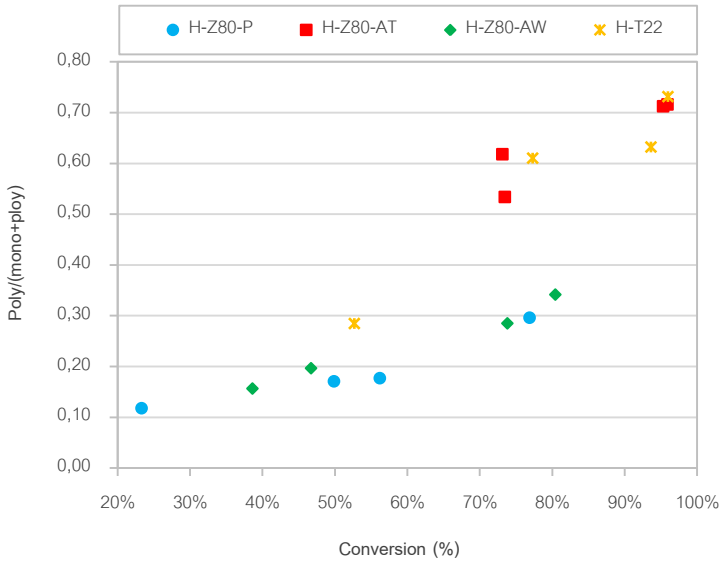

Figure 27: Ratio between the poly-branched FA yield and the total branched FA yield (mono-branched and ploy-branched FA) obtained during alkyl-isomerisation of oleic acid by modified and unmodified H-Z80 when tested at [..].% loading, compared to that obtained by the H-T22 catalyst. Both mono-branched and poly-branched FA yields are calculated as a percentage of the total monomer present in the product.

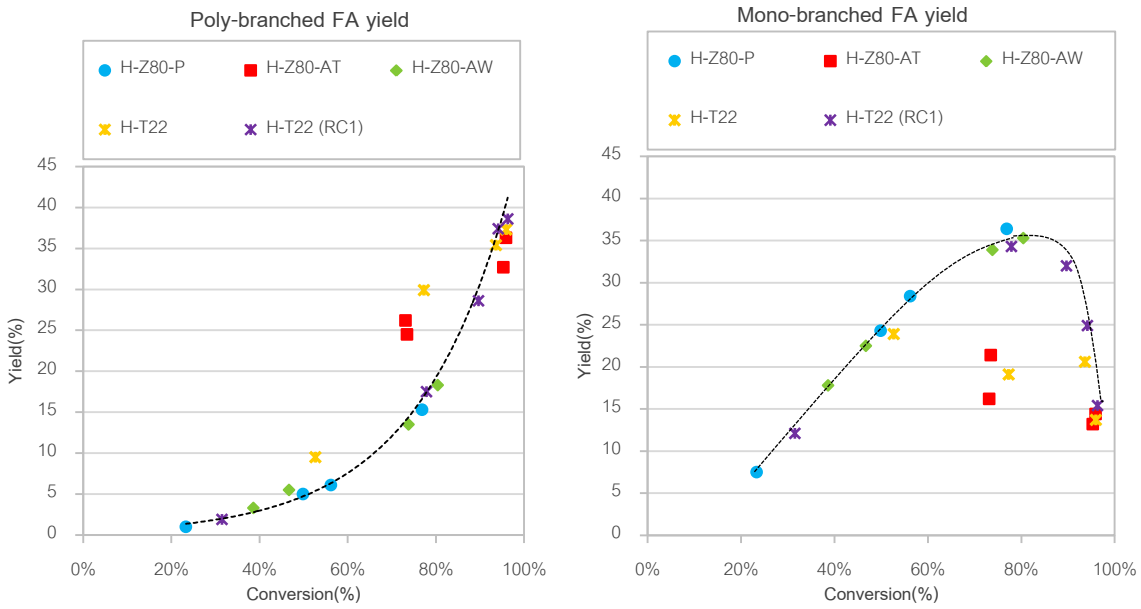

Figure 28: Poly-branched FA and mono-branched FA yield vs conversion, calculated as a percentage of the total converted monomer present in the product. All catalysts are tested with a [..]% loading in a mini-PARR autoclave with 25 g of feed, The H-T22 sample was also tested in a different reactor (RC1) at [..]. % loading and 800g of feed (✱) (see also section 4.4). The fitting line in a) is an exponential fit of the points from H-Z80-P, H-Z80-AW and H-T22(RC1)), while the trend line in b) do not represent any mathematical fitting, rather a guideline to clarify the trend of mono-branched yield growth and following decline after a certain conversion.

3.2.2. H-Z80, [..]. % loading

In the previously displayed experiments at [..]. % loading, the mesoporous [...] treated catalyst showed a big improvement in conversion compared to the untreated H-Z80-P (96% conversion reached, compared to the 60% of the parent catalyst). Since the H-T22 catalyst loading was set at [..]. %, it is of interest to verify the performance of the H-Z80-AT at such loading as well. For this reason, a second batch of [...] treated H-Z80 sample was prepared and tested. Furthermore, a third batch of [...] treated H-Z80 sample was made and subjected to a post [...] treatment. Due to the small amount obtained, this last sample could only be tested at [..]. % loading. To better understand the effect of the treatments one alkyl isomerisation experiment at [..]. % loading was also conducted with the parent zeolite. The results are reported in Figure 29.

[Confidential]

Figure 29: Conversion vs reaction time at [..]. % loading of a new batch of the modified H-Z80 sample which showed the best conversion in the experiments at [..]%, namely H-Z80-AT, compared to the current best material, H-T22. The H-Z80-AT+AW was also tested, since the small amount obtained during preparation of the catalyst did not allow for testing at higher loading. As a reference, one experiment was conducted at [..]. % loading with the parent H-Z80 catalyst. All the experiments were carried out with a catalyst weight loading of [..]% and 25 g of feed in a mini-PARR autoclave.

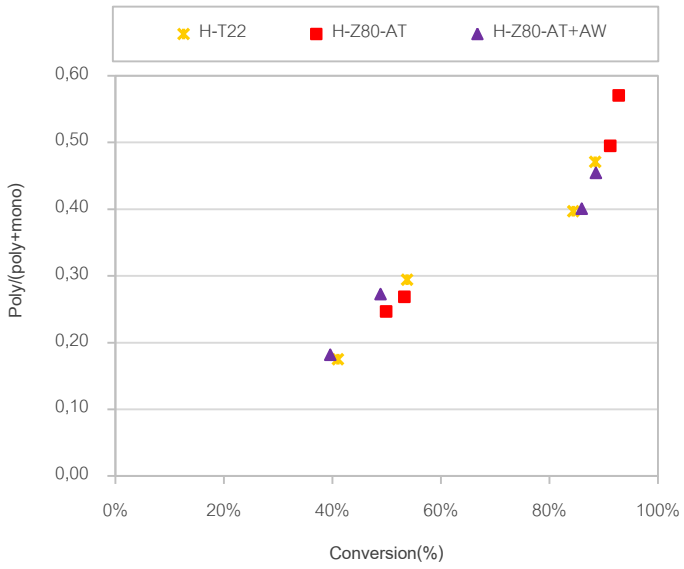

Figure 30: Ratio between the poly-branched FA yield and the total branched FA yield (mono-branched and ploy-branched FA). Both yields are calculated as a percentage of the total monomer present in the product when tested at [..]. % loading. All three catalysts give alkyl isomerisation products with a similar branching pattern at a specific conversion.

Again, the [...] treated sample (H-Z80-AT, in red) shows a significant improvement from the parent, to the point of exceeding the conversion obtained by the H-T22 sample (in yellow). Furthermore, the improvement from the parent zeolite brought by this treatment is even more accentuated than what was shown in the experiments at [..]. % loading (see Figure 26). Specifically, after 5.5h hours of reaction time the parent zeolite has only reached a conversion of 33%, while the [...] treated H-Z80 has achieved 91% conversion. After the same reaction time, the H-T22 has reached 84% conversion. Note that this H-Z80-AT sample belongs to a different batch than the one tested at [..]. % loading; therefore, it is likely that desilication was more efficient in the sample tested at [..]. % loading. This indicates that the treatment procedure still requires some further optimisation.

The ratio between the poly-branched FA in the product and the total amount of branched FA was again calculated for all samples and compared. These values are reported in Figure 30, plotted vs. the conversion percentage values of each specific catalyst, showing again that the branching pattern of the H-Z80 mesoporous sample is comparable to that of the H-T22 reference

The oleic acid conversion gives information about the overall activity of the catalyst. However, the desired product of the alkyl-isomerisation process is the branched FA. Therefore, it is interesting to also compare the branched FA yields obtained by the different catalysts, to have an indication of the yield that could be achieved. Furthermore, side reactions like oligomerisation can also occur in different measures, depending on specific characteristics of each catalyst. Both branched FA and oligomer yields obtained at [..]. % loading are reported in Figure 31 for the three H-T22, H-Z80-AT and H-Z80-AT+AW catalysts and the unmodified H-Z80-P, as a reference. All three catalysts give a branched FA yield of 58% after 5.5 h reaction time, compared to the 16% of the parent H-Z80-P zeolite. This further confirms the potential of the mesoporous H-Z80 catalyst obtained by [...] treatment. However, the modification of the catalyst brings also an increase in the oligomer yield, which is relatively higher than that obtained when employing H-T22 and the unmodified H-Z80-P (18% against 11% after 5.5h reaction time). Because NH_3-TPD analyses suggested that the H-T22 had higher EFAl concentration than the H-Z80-AT catalysts, it is presumed that such increase in oligomer yield for the [...] treated H-Z80-AT might be due to its high surface area. EFAl species only partially contribute to the Lewis acidity of the catalyst and, therefore, to the selectivity toward oligomerisation of a zeolite catalyst. In fact, H-T22 shows higher concentration of EFAl, but low oligomer yield. This could be due to its lower surface area, but it is also possible that the

manufacturer synthesis procedure involved steps to ensure a low concentration of Lewis sites, responsible for the oligomerisation reaction.

[Confidential]

Figure 31: Branched FA yield and oligomer yield obtained with the mesoporous H-Z80 catalysts, compared to the parent zeolite and the H-T22 reference.

3.2.3. H-Z23, [..]. % loading

A second commercial catalyst, H-Z23, was also subjected to the same modifications treatments. The H-Z23 parent zeolite has a lower Si/Al ratio than the H-Z80. Therefore, different strategies should be considered to obtain optimal mesoporosity and the same treatment is expected to have different consequences on the two catalysts. Figure 32 shows the conversions obtained by alkyl-isomerisation with the modified and unmodified H-Z23 catalysts, compared to the H-T22 zeolite performance. Unlike the H-Z80, the H-Z23 seems to be unaffected by the [...] treatment, while the two samples treated by [...], either alone or as a post wash following the [...] treatment procedure, show an improved conversion. However, the unmodified H-Z23-P catalyst already shows a conversion relatively close to that of the H-T22 catalyst at this loading. This has initially been ascribed to the similar Si/Al ratio between the two zeolites, hence similar acid sites concentration. In fact, the total NH_3 uptake test showed that these two samples have relatively high acidity. On the other hand, the modified H-Z23-AT+AW was found to uptake much lower NH_3 quantities, indicating a drastic decrease in the acidity of the H-Z23 due to the modification procedure. Nonetheless, some minor mesoporosity was also revealed by physisorption in the modified the modified H-Z23-AT+AW, which could explain the improvement in conversion of this catalyst compared to its parent H-Z23-P, despite the lower acidity.

[Confidential]

Figure 32: Conversion vs reaction time of the unmodified and modified H-Z23 samples, compared to H-T22. The [...] treated sample (H-Z80-AT, in red) shows no improvement from the parent, while the samples that were subjected to [...], alone or as a post-treatment to [...] treatment, show conversion similar to that of the H-T22 catalyst. All the experiments were carried out with a catalyst weight loading of [..]% and 25 g of feed in a mini-PARR autoclave.

3.2.4. H-Z23, [..]. % loading

The catalytic tests of the modified and unmodified H-Z23 zeolites show conversions close to that of the H-T22 catalyst, already in the parent H-Z23-P zeolite. On the contrary, when the catalysts are tested at a lower [..]. % loading, the differences between H-Z23 and H-T22 catalysts performances are significantly larger, as clearly represented in Figure 33. This dependence of performances on the catalyst loading is treated in the discussion (section 4.4).

For the scope of this project, however, the analyses of the catalyst behaviour at [..]. % loading is more interesting, being the reference H-T22 loading. Hence, from these results we can see that the modification procedures don't improve the H-Z23 catalyst performance to a desirable level. Nonetheless, the two samples that were subjected to [...] and [...] treatment followed by [...] show better conversion than the parent catalyst (66% conversion reached after 5.5h, compared to the 42% obtained by the parent catalyst). Since the desilication doesn't seem to have affected the catalyst performance (see experiment at [..]. % loading, Figure 32) and the two H-Z23-AW and H-Z23-AT+AW show very similar performance, it is likely that these last two samples are

not very different. However, a complete characterisation of the H-Z23-AT and H-Z23-AW samples should be done to check if this is actually the case. There is more known about the H-Z23-AT+AW catalyst; hence, a better analysis of its performance can be done. It is shown by NH_3-TPD that the total uptake is drastically reduced by the treatment, but physisorption analyses have revealed that only a marginal level of mesoporosity is also introduced. This might be the reason why, despite the acidity reduction, the conversion is somewhat enhanced. Furthermore, unlike the introduction of mesopores in the H-Z80 by [...] treatment, the treatment on H-Z23 results only in an enhancement of the branched FA yield, while the oligomer yield obtained is the same as for the parent H-Z23 (*not shown here*).

Although none of these samples can be considered as good candidates for industrial production, for completeness of analyses, the ratio between the poly-branched FA and the total branched FA has also been calculated. As represented in Figure 34, the product obtained by the H-T22 catalyst shows to be off-trend at conversion lower than 60%, which is already evidenced in the analyses of the H-Z80 catalyst performances. As for the product of the modified H-Z23 catalyst, the ratio values are more in line with the exponential trend.

[Confidential]

Figure 33: Conversion vs reaction time at [..]. % loading of the parent H-Z23 and modified catalysts that showed improved conversion, compared to H-T22. The modified H-Z23 catalysts give better conversion compared to their parent; however, they do not show the high conversion of the H-T22 catalyst, as it seemed to be the case when tested at [..]. % loading. All the experiments were carried out with a catalyst weight loading of [..]% and 25 g of feed in a mini-PARR autoclave.

[Confidential]

Figure 34: Ratio between the poly-branched FA yield and the total branched FA yield (mono-branched and ploy-branched FA) for the product obtained by the modified and unmodified H-Z23, compared to that obtained by the H-T22 catalyst, when tested at [..]. % loading. Both mono-branched and poly-branched FA yields are calculated as a percentage of the total monomer present in the product.

4. Discussion

4.1. H-T22 characteristics and effect of the modification treatments on NH_4-Z80

As clear from the results obtained by the alkyl-isomerisation tests with the modified and unmodified H-Z80 samples, the [...] treatment resulted in a catalyst with both conversion and branching pattern comparable to that of H-T22. The modification technique employed was reported in literature as the optimal method to introduce mesoporosity in catalysts with Si/Al ratio between 25 and 50, and the commercial NH_4-Z80 catalyst lies in this category. Physisorption analyses showed a significantly higher mesopore area in the H-Z80-AT sample when compared to its parent, confirming that the desilication by [...] treatment was indeed successful. However, the acidity of the so obtained catalyst was found to be much lower than the H-T22 reference zeolite. Furthermore, the H-T22 commercial zeolite did not show a significant level of mesoporosity compared to the HZ80-AT, while the presence of macropores could be deduced by physisorption data in both catalysts. Despite their differences in acidic and textural properties, the two catalysts showed both relatively good conversions and similar proportion between mono-branched and poly-branched FA in the obtained product of the oleic acid alkyl-isomerisation.

To help the discussion, a graphic representation of what is thought to be the particle structure of these two catalysts is shown in Figure 35. The H-T22 sample has relatively low microporosity (0.119 $cm^3 \cdot g^{-1}$), but small crystals ([…], as declared by the manufacturer) and high acid sites concentration (1.3 $mmol \cdot g^{-1}$ NH_3 uptake). These small crystals are expected to be closely packed together, forming inter-crystalline mesopores and macroporous voids, which also contribute to the ease of access of the reactants to the micropores. A marginal level of mesoporosity and discrete macroporosity were indeed revealed by physisorption analysis on this sample. Therefore, despite the relatively low microporosity and surface area, the overall accessibility to the acid active sites and their intrinsic high concentration, justify the good conversion obtained by such catalyst.

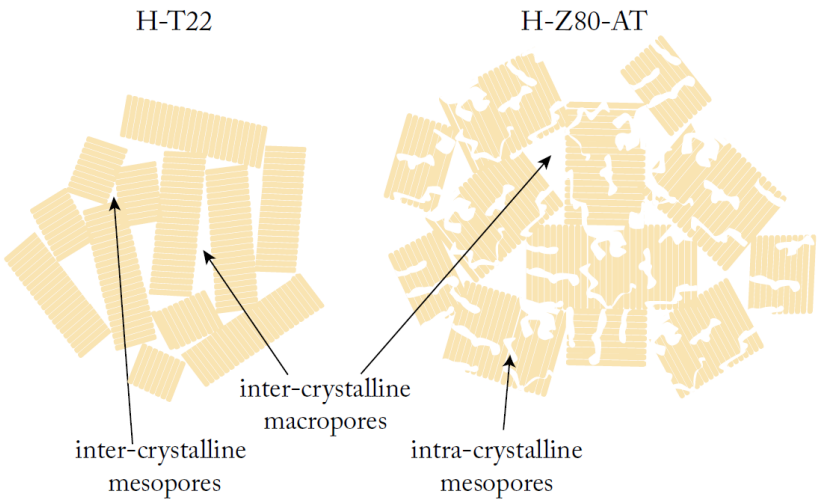

Figure 35: Graphic representation of the textural properties of the two H-T22 and H-Z80-AT catalysts, which showed similar conversions and branching pattern for the alkyl-isomerisation of oleic acid. The H-T22 has relatively small crystals ([…]), which are expected to be closely packed within a particle and, therefore, to have macroporous voids between crystallites and possibly also some level of inter-crystalline mesoporosity. The H-Z80-AT zeolite has relatively bigger crystals, although small enough to also potentially create inter-crystalline macropores when closely packed together. Furthermore, the [...] treatment has introduced intra-crystalline mesopores, enhancing greatly the accessibility to the active sites within the catalyst crystals.

On the other hand, the unmodified H-Z80-P catalyst has higher microporosity (0.160 $cm^3 \cdot g^{-1}$) than the H-T22, slightly bigger crystals ([…] average size), no significant mesoporosity and much lower acid concentration due to the higher Si/Al ratio, which explains the low activity compared to the H-T22 catalyst. Treating the catalyst with [...] solutions showed to reduce the acidity even further. However, it is clear that the treatment mainly removed silicon from the zeolite framework, successfully creating mesopores, greatly increasing the accessibility to the acidic active sites of the catalyst. Therefore, despite the lower intrinsic concentration of active sites of the H-Z80-AT catalyst when compared to the H-T22, their accessibility is enhanced to the point of obtaining a catalyst with conversions comparable to that of the highly acidic H-T22 catalyst

Furthermore, the [...] performed after the [...] treatment revealed to have an insignificant effect on the catalyst performance. According to the literature, desilication by [...] treatment might lead to partial removal of aluminium from framework positions, and a mild wash with an acidic solution could be useful in removing such extra-framework aluminium species.[14] These species are in fact likely to contribute to the oligomerisation of oleic acid. However, the NH_3-TPD profile of the H-Z80-AT catalyst showed no peak in the LT region. Although this peak has been ascribed to different species in literature, it is likely that EFAl species with weak Lewis acidity would cause TPD desorption in the LT region of the TPD profile. Therefore, it can be assumed that the H-Z80-AT sample had insignificant amounts of EFAl, probably thanks to the extensive rinsing, following the [...] treatment. For this reason, the [...] treatment on the desilicated catalyst did not have any beneficial effect. Furthermore, the conversion obtained by the H-Z80-AT+AW is somewhat lower than that obtained by the only [...] treated H-Z80-AT catalyst; it is possible that the lower conversion obtained is due to a less efficient desilication obtained while preparing the H-Z80-AT+AW batch. Otherwise, it is also probable that the [...] might have removed some of the framework aluminium species from the mesoporous catalyst, slightly diminishing the concentration of the Brønsted acid sites responsible for the alkyl-isomerisation reaction, thus causing the lower conversion. Furthermore, the oligomer yields obtained by the two catalysts were also comparable. Therefore, the [...] as a post-treatment on the desilicated sample does not seem to be the way to lower the oligomer selectivity, but might have a negative effect on the total acidity of the desilicated sample (although this should be confirmed by characterisation of the H-Z80-AT+AW sample).

The [...] alone also proved to increase the catalyst performances, but not as significantly as the [...] treatment. The H-Z80-AW sample was not characterised, so we can only speculate on the properties of this catalyst. It is possible that only a minor dealumination of the sample occurred, creating a marginal mesoporosity, which could be the reason for the improved conversion. Because the [...] was very mild and the parent zeolite had low Al content to start with, it is likely that the modification generated by this treatment might have affected only the external part of the catalyst particles. Furthermore, it is expected that the Brønsted acidity of the catalyst also decreased, due to the removal of framework Al. Therefore, if harsher acid treatment would be employed, it is not believed that beneficial effect would be encountered. However, the filtration of this catalyst from the product was perceived as much easier than any on the catalyst tested. Being a desirable feature, it would be interesting to investigate what gave this zeolite such property and verify if it could be transposed to more active catalysts.

4.2. Effect of the modification treatments on NH_4-Z23

As expected, when subjecting the commercial NH_4-Z23 catalyst to the same treatments as the NH_4-Z80, different results were obtained. This is related to the different characteristics of the two zeolites, starting from the very different Si/Al ratio. Furthermore, the textural properties of these two catalysts are also different. The H-Z23-P has smaller surface areas and larger crystals than the H-Z80-P (reported in literature to be below […] average size[63] against the […] of the H-Z80[52]). Therefore, despite its higher concentration of acid sites detected by NH_3-TPD (as expected from its much lower Si/Al ratio), the only slightly higher conversions

of the H-Z23-P can be addressed to the textural properties of its strictly microporous structure, which makes most acid sites difficult to access.

It is known from the literature that catalysts with high Al content are less susceptible to desilication by [...] treatment, due to the directing agent of the framework Al. This has been confirmed by our experiments. Although no characterisation of the [...] treated H-Z23-AT sample was performed, it is evident that no improvement for the alkyl-isomerisation reaction was introduced by this modification technique. Furthermore, extra-framework aluminium also inhibits Si extraction and NH_3-TPD analysis revealed that such species might be present on this commercial catalyst.

On the other hand, both H-Z23-AW and H-Z23-AT+AW showed better conversion than their parent zeolite. Due to the high Al content, it is predictable that even a mild [...] like that employed in this project, could remove some Al from the framework and bring changes to the sample properties. Both H-Z23-AW and H-Z23-AT+AW catalysts have similar performances, but only the H-Z23-AT+AW has been characterised by N_2 physisorption and NH_3-TPD. Therefore, we cannot exclude the possibility that the two catalysts might be very similar, if the [...] treatment had no significant effect in the H-Z23-AT+AW. Nonetheless, the experiments at [..]. % loading showed that these catalysts still have lower conversions than the H-T22 reference.

Nonetheless, this indicates that there is a margin of improvement also for zeolites with low Si/Al ratio. For comparison purposes, the modification procedures applied to H-Z80 and H-Z23 were kept the same, but it is known from literature that to obtain significant mesoporosity in zeolites with low Si/Al ratio, a harsher [...] treatment (0.5 M NaOH rather than 0.2 M) followed by post [...] should be employed.[14] It would be interesting to verify if such a treatment could result into a catalyst with improved performances for this application.

4.3. General reaction mechanism:

From the analyses of the alkyl-isomerisation products obtained by the different ZSM-5 catalysts, it is clear that the poly-branched and the mono-branched FA yields plotted against conversion followed different trends. Specifically, the poly-branched FA yield increases exponentially with the conversion. On the other hand, the mono-branched FA, which at the beginning of the reaction are always present in higher quantities than the poly-branched FA, increase in yield only to a certain point, before drastically decreasing at high conversion values. This is also the reason why the ratio between poly-branched and mono-branched FA increases with the reaction time and it is strictly related to the reaction conversion value.

A possible graphical explanation of the reaction steps behind these trends is represented in Figure 36. The trend of the poly-branched and mono-branched FA yield is also reported and divided into three phases (a, b and c) along the conversion. A zoom-in of the catalyst micropores, where the active sites are located, schematically shows the alkyl-isomerisation at different conversion phases. At the beginning of the reaction, the reactant mainly contains unbranched FA (principally oleic and elaidic acid -the trans isomer of oleic acid- and a small amount of poly-unsaturated FA). When an unsaturated FA molecule enters a micropore and reaches an active site, a mono-branched FA molecule desorbs. On the other hand, poly-unsaturated FA molecules that undergo isomerisation desorb from the micropore as poly-branched FA, due to the presence of two double bonds on the reactant molecules. However, the poly-unsaturated FA content in the feed is relatively low and cannot justify the poly-branched FA concentration that is found in the reaction product, already relatively high at early stages of the reaction. Hence, other reaction steps must be involved in the production of poly-branched FA. A possibility is that mono-branched FA re-enter the micropore and undergo a second isomerisation; moreover, it is also possible that some monounsaturated unbranched FA molecule reaches two active sites within the same pore and directly desorb as a poly-branched FA (the second carbocation being generated via hydrogen transfer). A situation where poly-branched FA can be produced in these two different ways can be written as:

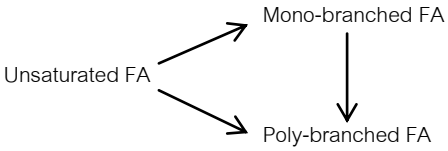

Eq. 4.1

Both processes are possible, but more detailed analyses should be conducted to verify which one of the two is predominant. Furthermore, for ease of discussion, this is a simplification of the reaction steps, which actually involve other side reactions, such as cracking. A real representation of the elementary reaction steps would be much more complex and making a quantitative kinetic analysis would require more data. Nonetheless, using this simplified set of reactions can be used to discuss the poly- and mono-branched FA yields trends in the alkyl-isomerisation reaction.

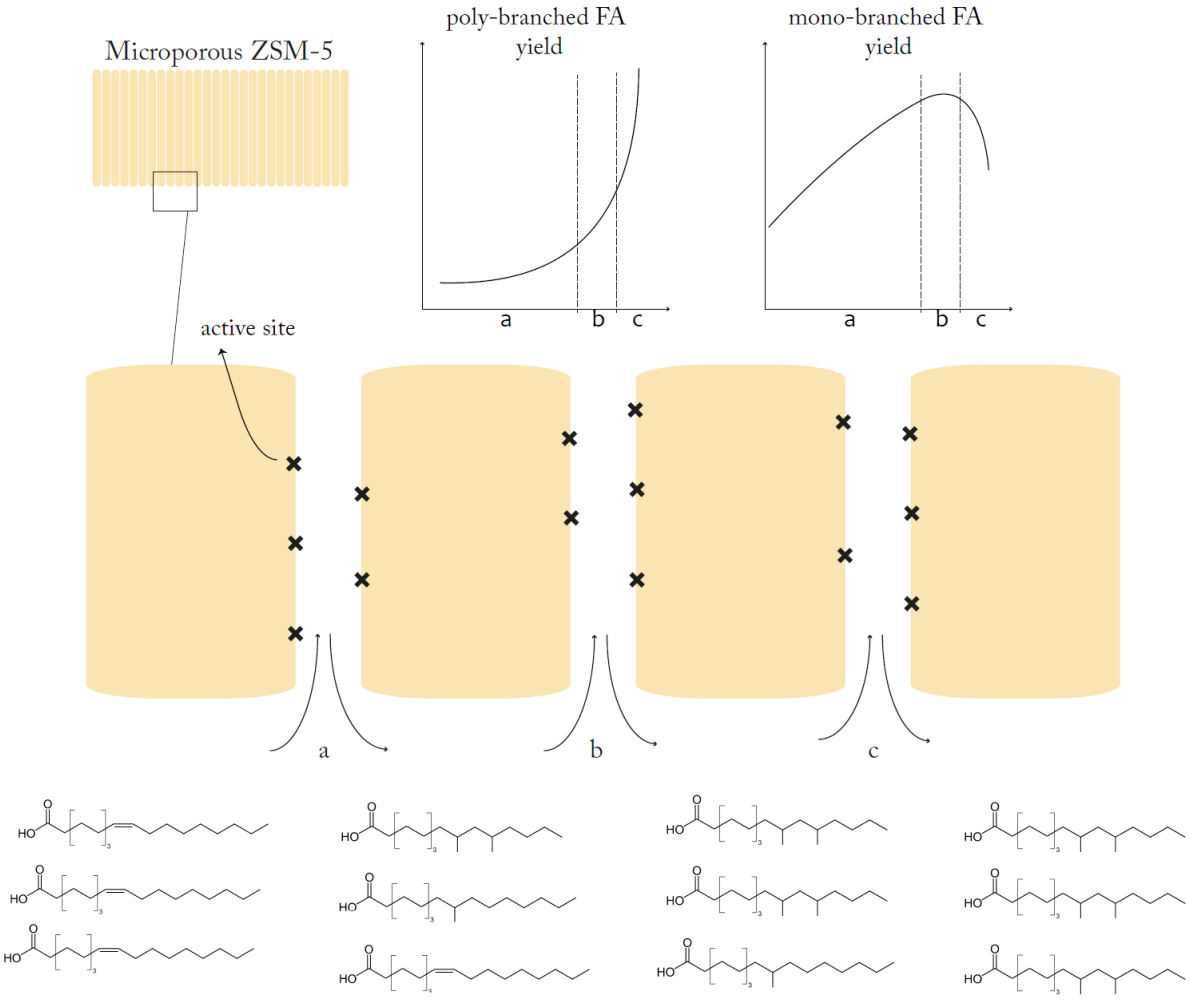

Figure 36: Graphical representation of the alkyl-isomerisation reaction steps to justify the curve trends of poly-branched and mono-branched FA yields vs conversion values. Note that in the reactant mixture also elaidic acid (trans-isomer of oleic acid) and small amounts of poly-unsaturated FA are present, but here omitted for simplification. Furthermore, only alkyl-isomerisation reactions are here represented, while other side reactions, such as oligomerisation or cracking are not considered.

Because the rate of a reaction is generally dependent on the reactants concentration, it is straightforward to understand why in phase (a), when the unsaturated FA concentration is high, both poly-branched and mono-branched FA yields are increasing.

In phase (b), on the other hand, the poly-branched FA yield still increases, while the mono-branched FA content seems to have reached a plateau. This could be explained if we assume that mono-branched FA do in fact re-enter the micropores to undergo

further isomerisation, acting as an intermediate to the production of poly-branched FA. Hence, mono-branched FA are produced by the reaction of unsaturated FA, but are also consumed to produce poly-branched FA.

Predictably, this brings to phase (c) where the mono-branched FA yield starts to decrease. This is due to the fact that at high conversion, the unsaturated FA concentration has drastically decreased, leading to slower rate of branched FA production. On the other hand, the mono-branched FA keep isomerising to poly-branched FA, justifying the still increasing yield of this product.

As presented in the results section, the H-T22 and H-Z80-AT catalysts seem to behave differently from the other catalysts. More specifically, the poly-branched FA yield in the product by them obtained is higher than expected at a certain conversion value, while the mono-branched FA yield is lower. The reason behind this behaviour is treated in the next section (4.4).

4.4. Uncharacteristic behaviour and H-T22 and H-Z80-AT outliers' data

During the catalytic tests performed for this project, several uncharacteristic behaviours were observed.

Early experiments performed with the reference H-T22 catalyst and the parent H-Z23 and H-Z80 catalysts in a different reactor (RC1) have shown much faster conversions than what is obtained when performing experiments at the same loading in the mini-PARR reactor (see Appendix 8.2). Note that only these catalysts could be tested in the RC1 reactor; because of its large capacity, high quantities of catalyst are needed for every reaction test, making impossible to test in this reactor the modified catalysts. Nonetheless, the higher conversions obtained when testing the catalysts in the RC1 compared to those achieved with the mini-PARR, suggest that the conditions of the mini-PARR reactor are not ideal for testing the ZSM-5 catalysts. This might be due to the fact that the reaction conditions for this reactor were in fact optimised for the alkyl-isomerisation reactions with a different type of catalyst, namely a commercial H-FER. At first, it was noted that the pressure reached during catalyst testing with H-ZSM-5 sample would range between 4.5 and 5.5 bars, while with the RC1 the pressure could be externally controlled and generally set at 8 bar. Hence, to exclude that this pressure difference might be the cause of the lower conversions obtained with the mini-PARR reactor, a series of experiments were run with the RC1 at different pressures (ranging from 4.5 to 11 bar) employing [..]. % loading of H-T22 catalyst. However, no difference in conversion was observed when the experiment was run at different pressures (see Appendix 8.3).

A parameter that also influences the conversion rate in diffusion limited reactions is the efficiency with which the reaction mixture is stirred. Efficient stirring of the mixture allows for higher chances for the catalyst and the reactant to enter into contact with each other. This allows for a better accessibility of the reactant to the pores of the catalyst and therefore, faster conversions. The removal of products which are desorbing from the pores is also important to maintain the reaction rate and this is also influenced by the stirring of the mixture. Therefore, it is likely that the stirring employed in the mini-PARR might not be ideal to allow for optimal mixing of the H-ZSM-5 catalysts with the reactant. Furthermore, it was verified that simply increasing the stirring speed is not enough to enhance stirring efficiency with this kind of stirrer (see Appendix 8.4). It is therefore assumed that a solution could be found by employing a different, more efficient, type of stirrer. These assumptions are supported by the fact that the RC1, which allows for alkyl isomerization testing with higher conversions, possess in fact a much more efficient stirring setup.

Nonetheless, all the experiments performed with the H-ZSM-5 catalysts samples were performed with the same parameters and are, therefore, comparable. Hence, the results obtained can still be considered a valid proof of the fact that hierarchical H-ZSM-5 might deliver the desired improvements in activity, which are the main scope of this project.

Moreover, other two observations were made during the catalytic testing. Specifically, the catalysts sample H-T22 and H-Z80-AT were found to give products with a higher poly-branched and a lower mono-branched FA yields than what should be expected for H-ZSM-5, as explained in section 4.3. However, as also anticipated in the results section 3.2.1, when the H-T22 catalyst was

tested in the RC1 reactor, the poly-branched and mono-branched FA yields were no longer outliers, but instead adhered to the trend (see Figure 28). This is an indication of the fact that such behaviour must be related to the poor stirring, somehow affecting only the (hierarchical) most active catalysts H-T22 and H-Z80-AT. Note that an inefficient stirring does negatively affect the conversion of all catalysts, but without influencing the ratio between poly-branched and mono-branched FA yield at a given conversion, as it is the case for the H-T22 and H-Z80-AT samples.

Furthermore, increasing the catalyst loading from [..]. % with these two catalysts did not seem to improve their performance as much as it did for the other purely microporous zeolites. A comparison of this effect on three different catalysts is shown in Figure 37. It is well known that a catalyst is used to increase the rate of a reaction and possibly directing it toward the desired product. By increasing the catalyst loading, the number of active sites accessible at the same time by the reactant molecules increases, therefore enhancing the reaction rate. A similar effect of increasing catalyst loading can also be obtained by enhancing the accessibility to the active sites of a catalyst, for example by introducing mesopores, as it is verified for our modified H-Z80-AT sample. Again, also the stirring efficiency has the same effect, since it influences the chances of catalyst and reactant to enter into contact with each other.

[Confidential]

Figure 37: Effect of catalyst loading on the alkyl-isomerisation conversion in time, for different catalysts. H-T22 (yellow), H-Z80-AT (red) and H-Z23-P (light blue).

From the characterisation of the samples and their performances during alkyl-isomerisation tests, it is known that these two catalysts are the only one with a significant second level of porosity (macropores in both and mesopores mainly in the H-Z80-AT sample). Although a complete analysis of the catalyst should be performed to have a full characterisation, we can already make some hypothesis on the peculiar behaviour of these two samples.

The presence of a second level of porosity is what gives such good conversion abilities to these catalysts, due to the fact that the active sites are more easily accessible to the reactant molecules. However, intra-crystalline mesopores like those found in the [...] treated H-Z80-AT sample, are expected to run through the entire length of the catalyst crystals and to be tortuous, rather than straight. The same could be said for the inter-crystalline macropores of the H-T22 sample. It is true that these bigger pores facilitate the access to the micropores within the catalyst particles/crystals. However, diffusion of the reactant molecules through these pores and of the product molecules from the pore to the outer surface also takes time, especially for long and tortuous paths (see *Thiele modulus* definition in section 1.4, Figure 6). Hence, even though the presence of mesopores increases the accessibility of the reactant to more active sites, if the stirring conditions are poor, the diffusion of both reactants and products through the mesopores remains inefficient.

A schematic of the different diffusion limitations between purely microporous and hierarchical zeolites is represented in Figure 38. The diffusion of the reactant is divided into three steps: *a*- toward the catalyst surface, *b*- within the micropore and *c*- within the mesopores. Note that the same opposite path is also followed by the product, with analogue diffusion limitation (if not higher, due to the bulkier nature of branched FA), indicated in the figure as a_1, b_1 and c_1. In purely microporous catalysts, the stirring efficiency influences step *a* (and a_1), while *b* (and b_1) is influenced on a smaller extent by it, while being mainly dependent on the relative dimension of the reactant (for *b*) and the product (for b_1) to that of the micropore. On the other hand, in hierarchical zeolites, the stirring efficiency also influences to a certain extent the diffusion through the mesopores (*c* and c_1). During the reaction, some of the FA reactant molecules are diffusing through the micropores accessible from the outer surface and undergo isomerisation reaction, as depicted in Figure 36. However, a great part of the unsaturated FA molecules diffuses through the

mesopores and isomerise within the micropores accessible from the mesopore. Because of the length and tortuosity of these pores and the poor stirring, the diffusion through the mesopores is relatively slow, especially when stirring is not efficient. Due to the slow diffusion of step c_1, once mono-branched FA have been formed, they have high chances to re-enter a micropore while diffusing through the mesopore, and further react to form a poly-branched FA. This could explain why the product obtained with these two samples contained higher poly-branched FA amounts and lower mono-branched FA content than expected at a given conversion, according to the H-ZSM-5 trend of the other microporous zeolites. On the other hand, when stirring is efficient (as it is the case in the RC1 reactor), the diffusion *a* -to the reactant from the mixture to the external surface of the catalyst- and diffusion *c* -from the mesopore entrance to the inside of the mesopore- are comparable. This justifies why the product obtained while testing the H-T22 in the RC1 has indeed poly-branched and mono-branched FA yield in the expected range (see Figure 28).

Furthermore, while performing catalyst testing at [..]. % loading with these two hierarchical zeolites, the catalyst was found to be agglomerated at the bottom of the reactor vessel at the end of the reaction. In particular, the H-Z80-AT catalyst was observed to form considerably big lumps. This also shows that inefficient stirring affects these catalysts more, justifying why conversions are not greatly improved by increasing catalyst loading.

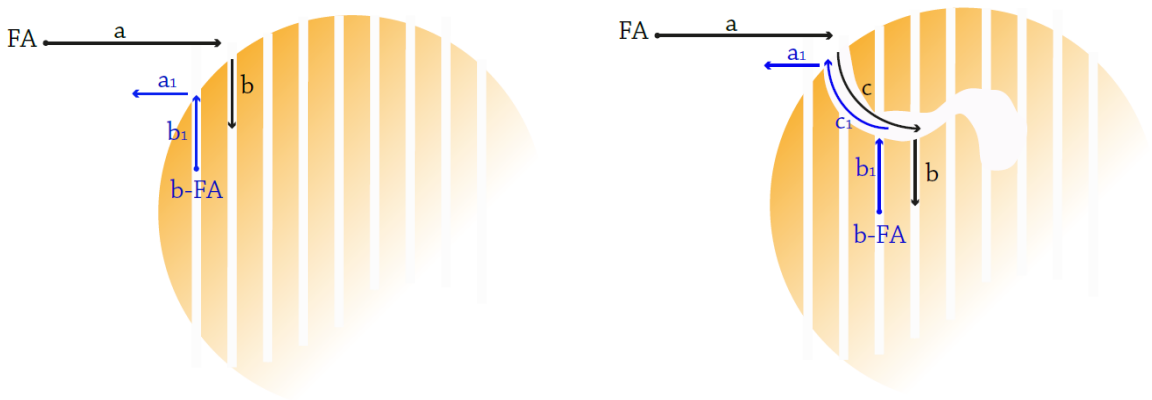

Figure 38: Diffusion steps taking place in microporous and hierarchical zeolites. First, the FA reactant molecule needs to diffuse from the mixture to the catalyst surface, where they enter micropores or mesopores (a). In purely microporous catalysts, the FA molecules diffuse through the micropore (b) and undergo reaction. If mesopores are present, some FA reactant molecules also diffuse through the tortuous mesopore (c) before reaching a micropore within the catalyst crystal. The products formed (b-FA) then diffuse back to the reaction mixture outside the catalyst particle through an opposite path, indicated in figure in blues as a_1, b_1 and c_1.

5. Conclusions

This project investigated the potential benefits of employing hierarchical ZSM-5 catalysts for the alkyl-isomerisation reaction of unsaturated fatty acids. The aim was to find an improved isomerisation catalyst. In order to obtain hierarchical zeolites, two commercial ZSM-5 catalysts with different Si/Al ratio (NH_4-Z80 with Si/Al=40 and NH_4-Z23 with Si/Al=11.5), were subjected to a series of top-down modification techniques, namely [...] treatment (AT), mild [...] (AW) and a combination of the two (AT+AW).

From the physisorption data, it is clear that the [...] treatment was successful in introducing mesopores in the NH_4-Z80 catalyst. The effect of a better accessibility to the active sites of the zeolites, due to the presence of mesopores, is clearly shown in the conversion improvement from the parent (H-Z80-P) to the modified H-Z80-AT catalyst performance (see Figure 39). The improvement was such that, despite possessing a much lower total acidity, the catalyst outperformed the H-T22 reference catalyst (91% conversion reached after 5.5h reaction time against the 84% obtained with the H-T22 and 35% with the unmodified H-Z8-P). These data were obtained by testing the catalysts in a mini-PARR reactor with non-optimal conditions. Therefore, these values are underestimating the conversion that could be obtained in an optimised reactor. Nonetheless, the catalytic tests were all conducted within the same system and with equal conditions, making the comparison of the catalyst performances still valid.

[Confidential]

Figure 39: Conversion vs time of the alkyl-isomerisation of FA obtained with [..]. % loading of H-Z80-P, H-Z80-AT and H-T22. The improvement brought by the [...] treatment is such that the H-Z80-AT catalyst outperformed the H-T22. A graphical representation of what is assumed to be the catalysts particle characteristics is represented on the right. H-Z80-P has relatively big crystals, poor accessibility to the active sites within the particle and low concentration of active acid sites. The modified H-Z80-AT performance improvement is justified by the great enhancement of active sites accessibility thanks to mesoporosity introduction. The H-T22 catalyst performance is due to its smaller crystals, which give a rather good accessibility to its active sites, present in high concentration.

The other modification procedures were not as effective on NH_4-Z80. The [...] seemed to improve the catalyst conversion, but only to a marginal level. Considering the physisorption data on this modified sample (H-Z80-AW), it is assumed that such modification only affected the external surface of the catalyst crystallite, increasing marginally the accessibility to the acid sites and, therefore, only slightly improving its performance. However, it is also expected that a harsher [...] would remove higher quantities of Al, reducing drastically the amount of Brønsted acid sites and, therefore, possibly being counterproductive.

The [...] on the [...] treated sample might have had the same effect, i.e. reducing the Brønsted acidity of the catalyst. In fact, the catalytic test of this modified zeolite (H-Z80-AT+AW) showed lower conversion compared to the solely [...] treated one (H-Z80-AT). However, it is not excluded that the poorer performance might have been due to a less efficient desilication by the [...] treatment, since the two samples were prepared starting from two different batches.

Furthermore, the results obtained during this project confirmed that different catalysts require different modification techniques, as preliminary literature research suggested. This was established when subjecting the second commercial catalyst (NH_4-Z23) to the same modification procedures applied on the NH_4-Z80 and experiencing very different results. Due to the low Si/Al ratio of NH_4-Z23, [...] treatment had no effect on the catalyst performance. This was expected since a high concentration of Al in the zeolite framework prevents Si extraction.[49] Furthermore, species like extra-framework aluminium also inhibit Si extraction and NH_3-

TPD analysis revealed that such species might be present in this commercial catalyst. On the contrary, the [...] did improve catalyst conversion, although not in a sufficient way. This might be due to an only very external mesoporosity introduced by selective aluminium extraction from the catalyst framework. Harsher conditions might lead to higher mesoporosity, although amorphisation of part of the catalyst might also occur. Furthermore, removal of Al inevitably reduces the concentration of Brønsted acid sites. Further investigation should be conducted to verify if there is still a margin of improvement for introducing mesopores in this catalyst by acid leaching without affecting its acidity too far.

The combination of [...] treatment and subsequent [...] was reported in literature to be an efficient way to introduce mesopores in low Si/Al ratio zeolite. However, the sample subjected to such treatments (H-Z23-AT+ZW) had very similar conversion to that of the simply [...]ed sample (H-Z80-AW). This suggested that the [...] treatment had probably no effect on this catalyst and the two H-Z23-AW and H-Z23-AT+AW modified zeolites might not be very different.

It can be concluded that the accessibility of the catalyst active sites is of extreme importance for the alkyl-isomerisation of FA. The results of this project showed that introducing mesopores in commercial catalysts with post-modification techniques is a valid way to enhance active sites accessibility in ZSM-5 zeolites. One hierarchical sample was obtained, by [...] treatment of an NH_4-HZ80 commercial catalyst, whose conversion outperformed that of H-T22. Although far from providing an industrially viable catalyst, these results show that the solution could be found in a zeolite with hierarchical porosity. It is in fact hypothesised that the reason behind the good performances of H-T22 catalyst lies in its textural properties, i.e. small crystals with inter-crystalline macroporosity, which allow for a good accessibility to its high concentration of acid sites (see Figure 39).

6. Outlook

During this project, it was successfully shown that introducing mesopores by modification treatments on commercial ZSM-5 zeolite could provide an answer to the search for an improved isomerisation catalyst. However, in order to find a definitive solution, further investigations should be conducted. Firstly, it is believed that a wider screening of modification techniques and optimisation of the most promising ones, might lead to hierarchical catalysts with higher conversion than those obtained in this project. Secondly, a better characterisation of the product composition is also considered necessary, to verify how it compares to the standard ISAC. Finally, estimating the cost of modifying a commercial catalyst on large-scale is also essential for commercial considerations. This outlook provides some suggestions on how these three aspects should be approached, although mainly focusing on the optimisation of the modification procedures.

Optimisation of modification techniques:

Due to the short length of the project, it was not possible to do a complete screening of modification techniques or to optimise the procedures that were shown as promising by the results obtained. For instance, it would be interesting to verify if the desilication by [...] treatment of the H-Z80 sample could be further improved, being the treatment adopted during this project with most successful results. The conditions of the treatment were chosen according to literature findings showing such conditions as optimal. However, it is possible that different conditions or different [...] solutions might lead to zeolites with better performance, specifically for the alkyl-isomerisation reaction. Furthermore, as suggested by the results obtained with different batches of [...] treated samples, it is possible that the reproducibility of the treatment might be lower than expected. This could be due to the relatively short time of the treatment stage in itself. Therefore, treatments with a lower concentration of NaOH and longer times should be tested, in order to verify if better reproducibility can be obtained. Furthermore, although the final calcination step of the modified catalysts was performed by all the studies reported in literature, one publication was found which claimed that avoiding the calcination step after [...] treatment might lead to catalysts with better characteristics. Specifically, it was reported that [...] treated ZSM-5 which were subsequently subjected to [...], but no calcination, would have higher concentrations of Brønsted acid sites and lower amounts of Lewis sites compared to the same catalyst which was calcined.[69] A catalyst with lower Lewis acidity would be highly desirable for the alkyl-isomerisation of FA, since it would give lower oligomerisation yields. As seen in the results of this project, the H-Z80 sample which was modified by [...] treatment and [...] still gives relatively high yields of oligomer products. Hence, it would be interesting to verify these literature results and see the effect of avoiding the calcination step on catalyst performance.

On the other hand, the modifications techniques applied to the H-Z23 catalyst did not bring sufficient improvement to introduce mesopores in low Si/Al ratio ZSM-5 zeolites, although literature suggested that [...] treatment followed by a mild [...] is a valid technique.[14] According to these literature findings, however, harsher [...] treatment should be performed before subjecting the catalyst to [...]. Hence, it would be interesting to verify if this is the case for the specific low Si/Al ratio catalyst employed during this project. However, the NH_3-TPD profile of the untreated H-Z23-P sample shows a relatively intense band in the low-temperature region, which might indicate the presence of extra-framework Al, possibly due to steaming performed on the catalyst by the manufacturer. In fact, it is known that such species also inhibits silicon extraction; hence, this might also have contributed to the inefficient mesopore formation in this catalyst.[8,10] If further characterisation of the sample would confirm the presence of

extra-framework Al, an option to consider would be a pre-treatment with oxalic acid, in order to remove these species and allow for a more efficient mesopores introduction.

Catalysts and product characterisation:

Moreover, the limited means available on site did not allow for a complete characterisation of all the catalysts obtained. A better understanding of the effect of the modification techniques on catalyst properties is essential in the research of an optimal procedure to obtain a catalyst with sufficient mesoporosity and adequate acidic properties for the alkyl-isomerisation reaction. Besides analysing the remaining catalyst by N_2 physisorption and NH_3-TPD, further analyses should be performed on all samples. For instance, studying the acidity of the catalysts by FTIR analyses with molecule probes like pyridine has been used in literature to identify and quantify different acid sites in ZSM-5 catalysts.[12,34,56,69,70] This technique allows for quantitative analyses and identification of acid sites nature and is, therefore, more useful than NH_3-TPD data. Furthermore, ^{29}Si and ^{27}Al Magic Angle Spinning (MAS) NMR has been widely used in literature, since it allows for identification of differently coordinated Si and Al species. Hence, performing this analysis would provide valuable information on the framework of a modified catalyst, for example when verifying the presence of extra-framework aluminium species.[56,62,69,71] Moreover, in addition to the physisorption data, subjecting the samples to SEM and TEM analyses would give a clearer picture of the samples morphology, giving a more precise illustration of the mesopores introduced. Another interesting analyses method that could be performed as complementary to N_2 physisorption is mercury-intrusion porosimetry.[72] This technique could be helpful in providing information on the presence of macropores, which we expect to be beneficial also in enhancing the accessibility to the acid sites within a catalyst particle.

Although secondary to the scope of this project, further GC analysis of the reaction products would be interesting to properly analyse its composition and compare it to the standard ISAC. It is known that in the product obtained by H-ZSM-5 both mono- and poly-branched FA are present. However, several isomers with the branch located at different positions occur. In fact, in the GC of the hydrogenated product reported in the methods section, it was evident that different mono and poly-branched species were eluted (Figure 20). A technique that could be used for this purpose, allowing for a better identification of the GC peaks of a mixture of branched-chain FA isomers, would be to first hydrogenate the product and then convert it to picolinyl ester derivatives. In this way, the chromatogram of the picolinyl esters gives a better separation of the branched isomers, allowing for identification of the branching positions. This technique was reported by Ngo et al., employed by them for the characterisation of alkyl-isomerisation product obtained with an H-FER catalyst.[4]

7. Bibliography

(1) Barrett, F. O.; Goebel, C. G.; Peters, R. M. Process of Dimerizing Monounsaturated Fatty Acids. US2793219, 1957.

(2) Myers, L. D.; Goebel, C. G.; Barrett, F. O. Polymerization of unsaturated Fatty Acids. US2955121, 1960.

(3) Myers, L. D.; Goebel, C. G.; Barrett, F. O. Process for Polymerizing Unsaturated Fatty Acids. US3076003, 1960.

(4) Ngo, H. L.; Nunez, A.; Lin, W.; Foglia, T. A. *Eur. J. Lipid Sci. Technol.* **2007**, *109* (3), 214–224.

(5) Wiedemann, S. C. C.; Stewart, J. A.; Soulimani, F.; van Bergen-Brenkman, T.; Langelaar, S.; Wels, B.; de Peinder, P.; Bruijnincx, P. C. A.; Weckhuysen, B. M. *J. Catal.* **2014**, *316*, 24–35.

(6) Wiedemann, S. C. C.; Ristanovic, Z.; Whiting, G. T.; ReddyMarthala, V. R.; Korger, J.; Weitkamp, J.; Wels, B.; Bruijnincx, P. C. A.; Weckhuysen, B. M. *Chem. Eur. J.* **2016**, *22*, 99–210.

(7) Ngo, H. L. *Eur. J. Lipid Sci. Technol.* **2014**, *116*, 645–652.

(8) Groen, J. C.; Peffer, L. A. A.; Moulijn, J. A.; Pérez-Ramírez, J. *Chem. - A Eur. J.* **2005**, *11*, 4893–4994.

(9) Wang, J.; Groen, J. C.; Yue, W.; Zhou, W.; Coppens, M.-O. *J. Mater. Chem.* **2008**, *18*, 468–474.

(10) Groen, J. C.; Moulijn, J. A.; Pérez-Ramírez, J. *Microporous Mesoporous Mater.* **2005**, *87* (2), 153–161.

(11) Groen, J. C.; Moulijn, J. A.; Pérez-Ramírez, J. *J. Mater. Chem.* **2006**, *16*, 2121–2131.

(12) Milina, M.; Mitchell, S.; Michels, N.-L.; Kenvin, J.; Pérez-Ramírez, J. *J. Catal.* **2013**, *308*, 398–407.

(13) Milina, M.; Mitchell, S.; Crivelli, P.; Cooke, D.; Pérez-Ramírez, J. *Nat Commun* **2014**.

(14) Verboekend, D.; Mitchell, S.; Milina, M.; Groen, J. C.; Perez-Ramirez, J. *J. Phys. Chem. C* **2011**, *115* (29), 14193–14203.

(15) Zhang, Z. C.; Dery, M.; Zhang, S.; Steichen, D. *J. Surfactants Deterg.* **2004**, *7* (3), 211–215.

(16) Gunstone, F. D. *Fatty Acid and Lipid Chemistry*; Springer US: Boston, MA, 1996.

(17) Haase, K. D.; Heynen, A. J.; Laane, N. L. M. *Lipid / Fett* **1989**, *91* (9), 350–353.

(18) Ngo, H. L.; Dunn, R. O.; Sharma, B.; Foglia, T. A. *Eur. J. Lipid Sci. Technol.* **2011**, *113* (2), 180–188.

(19) Schneider, M. P. *J. Sci. Food Agric.* **2006**, *86*, 1769–1780.

(20) Wiedemann-Tollington, S. C. C. Ferrierite-Catalysed Branching of Unsaturated Fatty Acids, Utrecht University, 2015.

(21) Vetter, W.; Wegner, I. *Chromatographia* **2009**, *70* (1-2), 157–164.

(22) MacDonald, R. C.; MacDonald, R. I. *J. Biol. Chem.* **1988**, *263* (21), 10052–10055.

(23) Ehara, T. Y.; Yamaguchi, K. Trehalose Fatty Acid Ester Composition. EP 2165712A1, 2008.

(24) Guerrero, A. A.; Klepacky, T. C. Sunscreen composition. 0681830A1, 1995.

(25) Cejka, J.; Corma, A.; Zones, S. *Zeolites and Catalysis: Synthesis, Reactions and Applications*; 2010; Vol. 1-2.

(26) O'Young, C.-L.; Pellet, R. J.; Casey, D. G.; Ugolini, J. R.; Sawicki, R. A. *J. Catal.* **1995**, *151*, 467–469.

(27) Lee, S. H.; Shin, C. H.; Hong, S. B. *J. Catal.* **2004**, *223* (1), 200–211.

(28) Tomifuji, T.; Abe, H.; Matsumura, .; Sakuma, Y. Process for the Preparation of Branched Chain Fatty Acids and Alkyl Esters Thereof. 5677473, 1997.

(29) Hodgson, W. R.; Koetsier, W. T.; Lok, C. M.; Roberts, G. Fatty Acids Isomerization. 5856539, 1999.

(30) Van Bergen-Brenkman, T.; Rashidi-Hamrahlou, N.; Wels, B. Process for producing monobranched fatty acids or alkyl esters thereof. WO2014064418A2, 2014.

(31) Ngo, H. L.; Hoh, E.; Foglia, T. A. *Eur. J. Lipid Sci. Technol.* **2012**, *114* (2), 213–221.

(32) Ngo, H. L. *Lipid Technol.* **2014**, *26* (11-12), 246–248.

(33) Lei, X.; Jockusch, S.; Ottaviani, M. F.; Turro, N. J. *Photochem. Photobiol. Sci.* **2003**, *2* (11), 1095–1100.

(34) Pérez-Ramírez, J.; Christensen, C. H.; Egeblad, K.; Christensen, C. H.; Groen, J. C. *Chem. Soc. Rev.* **2008**, *37* (11), 2530–2542.

(35) Fernandez, C.; Stan, I.; Gilson, J.-P.; Thomas, K.; Vicente, A.; Bonilla, A.; Pérez-Ramírez, J. *Chem. Eur. J.* **2010**, *16*, 6224–6233.

(36) Koekkoek, A. J. J.; Xin, H.; Yang, Q.; Li, C.; Hensen, E. J. M. *Microporous Mesoporous Mater.* **2011**, *145* (1-3), 172–181.

(37) Zhang, B.; Li, X.; Wu, Q.; Zhang, C.; Yu, Y.; Lan, M.; Wei, X.; Ying, Z.; Liu, T.; Liang, G.; Zhao, F. *Green Chem.* **2016**, 3315–3323.

(38) Serrano, D. P.; Escola, J. M.; Sanz, R.; Garcia, R. a.; Peral, a.; Moreno, I.; Linares, M. *New J. Chem.* **2016**, *40*, 4206–4216.

(39) Scott Fogler, H.; Szent-Gyorgyi, A. In *Elements of Chemical Reaction Engineering*; 2006; pp 813–866.

(40) Egeblad, K.; Christensen, C. H.; Kustova, M.; Christensen, C. H. *Chem. Mater.* **2008**, *20* (3), 946–960.

(41) Wei, Y.; Parmentier, T. E.; de Jong, K. P.; Zecevic, J. *Chem Soc Rev* **2015**, *44*, 7234–7261.

(42) Li, K.; Valla, J.; Garcia-Martinez, J. *ChemCatChem* **2014**, *6*, 46–66.

(43) Möller, K.; Bein, T. *Chem Soc Rev* **2013**, *42*, 3689–3707.

(44) Dessau, R. M.; Valyocsik, E. W.; Goeke, N. H. *Zeolites* **1992**, *12* (7), 776–779.

(45) Groen, J. C.; Bach, T.; Ziese, U.; Paulaime-Van Donk, A. M.; De Jong, K. P.; Moulijn, J. A.; Pérez-Ramírez, J. *J. Am. Chem. Soc.* **2005**, *127* (31), 10792–10793.

(46) Ogura, M.; Shinomiya, S. Y.; Tateno, J.; Nara, Y.; Nomura, M.; Kikuchi, E.; Matsukata, M. *Appl. Catal. A Gen.* **2001**, *219*, 33–43.

(47) Groen, J. C.; Peffer, L. A. A.; Moulijn, J. A.; Pérez-Ramírez, J. *Microporous Mesoporous Mater.* **2004**, *69*, 29–34.

(48) Groen, J. C.; Peffer, L. A. A.; Moulijn, J. A.; Pérez-Ramírez, J. *Colloids Surfaces A Physicochem. Eng. Asp.* **2004**, *241*, 53–58.

(49) Groen, J. C.; Jansen, J. C.; Moulijn, J. A.; Pérez-Ramírez, J. *J. Phys. Chem. B* **2004**, *108* (35), 13062–13065.

(50) Groen, J. C.; Caicedo-Realpe, R.; Abelló, S.; Pérez-Ramírez, J. *Mater. Lett.* **2009**, *63* (12), 1037–1040.

(51) Groen, J. C.; Hamminga, G. M.; Moulijn, J. A.; Pérez-Ramírez, J. *Phys. Chem. Chem. Phys.* **2007**, *9* (34), 4822.

(52) Meunier, F. C.; Verboekend, D.; Gilson, J.-P.; Groen, J. C.; Pérez-Ramírez, J. *Microporous Mesoporous Mater.* **2012**, *148*, 115–121.

(53) Christensen, C.; Johannsen, K.; Tornqvist, E.; Schmidt, I.; Topsoe, H.; Christensen, C. *Catal. Today* **2007**, *128* (3-4), 117–122.

(54) Bjørgen, M.; Joensen, F.; Spangsberg Holm, M.; Olsbye, U.; Lillerud, K.-P.; Svelle, S. *Appl. Catal. A Gen.* **2008**, *345* (1), 43–50.

(55) Holm, M. S.; Svelle, S.; Joensen, F.; Beato, P.; Christensen, C. H.; Bordiga, S.; Bj??rgen, M. *Appl. Catal. A Gen.* **2009**, *356* (1), 23–30.

(56) Gil, B.; Mokrzycki, L.; Sulikowski, B.; Olejniczak, Z.; Walas, S. *Catal. Today* **2010**, *152* (1-4), 24–32.

(57) Groen, J. C.; Moulijn, J. A.; Pérez-Ramírez, J. *Ind. Eng. Chem. Res.* **2007**, *46*, 193–4201.

(58) Milina, M.; Mitchell, S.; Cooke, D.; Crivelli, P.; Pérez-Ramírez, J. *Angew. Chemie Int. Ed.* **2015**, *54* (5), 1591–1594.

(59) Van Donk, S.; Janssen, A. H.; Bitter, J. H.; de Jong, K. P. *Catal. Rev.* **2003**, *45* (2), 297–319.

(60) Müller, M.; Harvey, G.; Prins, R. *Microporous Mesoporous Mater.* **2000**, *34* (2), 135–147.

(61) You, S. J.; Park, E. D. *Microporous Mesoporous Mater.* **2014**, *186*, 121–129.

(62) Dapsens, P.; Mondelli, C.; Pérez-Ramírez, J. *ChemSusChem* **2013**, *6*, 831–839.

(63) Brown, R. *Catalytic Processing of Whole Algal Biomass into Aromatics and Ammonia*; 2015.

(64) Hidalgo, C. V.; Itoh, H.; Hattori, T.; Niwa, M.; Murakami, Y. *J. Catal.* **1984**, *85* (2), 362–369.

(65) Topsoe, N. Y.; Pedersen, K.; Derouane, E. G. *J. Catal.* **1981**, *70* (1), 41–52.

(66) Woolery, G. L.; Kuehl, G. H.; Timken, H. C.; Chester, a. W.; Vartuli, J. C. *Zeolites* **1997**, *19* (4), 288–296.

(67) Barthos, R.; Lónyi, F.; Onyestyúk, G.; Valyon, J. In *Solid State Ionics*; 2001; Vol. 141-142, pp 253–258.

(68) Lónyi, F.; Valyon, J. *Microporous Mesoporous Mater.* **2001**, *47* (2-3), 293–301.

(69) Mitchell, S.; Milina, M.; Verel, R.; Hernández-Rodríguez, M.; Pinar, A. B.; McCusker, L. B.; Pérez-Ramírez, J. *Chem. - A Eur. J.* **2015**, *21*, 14156–14164.

(70) Xue, Z.; Zhang, T.; Ma, J.; Miao, H.; Fan, W.; Zhang, Y.; Li, R. *Microporous Mesoporous Mater.* **2012**, *151*, 271–276.

(71) Yoo, W. C.; Zhang, X.; Tsapatsis, M.; Stein, A. *Microporous Mesoporous Mater.* **2012**, *149*, 147–157.

(72) Groen, J. C.; Brouwer, S.; Peffer, L. A. A.; Pérez-Ramírez, J. *Part. Part. Syst. Charact.* **2006**, *23*, 101–106.

(73) Huangfu, J.; Mao, D.; Zhai, X.; Guo, Q. *Appl. Catal. A Gen.* **2016**, *520*, 99–104.

(74) Zhang, X.; Lin, L.; Zhang, T.; Liu, H.; Zhang, X. *Chem. Eng. J.* **2016**, *284*, 934–941.

(75) Wei, Z.; Xia, T.; Liu, M.; Cao, Q.; Xu, Y.; Zhu, K.; Zhu, X. *Front. Chem. Sci. Eng.* **2015**, *9* (4), 450–460.

8. Appendix

8.1. Literature data on ZSM-5 modification techniques

[...]

8.2. RC1/mini-PARR comparison

The mini-PARR reactor, employed in this project for the catalytic testing of the modified samples, was optimised with a different catalyst, FER. Lower conversions than expected were in fact obtained with this reactor. A second reactor with larger capacities and a better possibility of parameters control is also available on site. However, since very small quantity of catalysts were prepared for each of the modified samples of this project, its employment was not possible. The only ZSM-5 samples available in sufficient quantities were the H-T22 reference and the parent of the commercial catalyst, H-Z80-P and H-Z23-P. Therefore, tests on the H-T22 and the H-Z80-P were also performed with the RC1 reactor. The results are shown in Figure 40. Clearly, the conversions obtained when testing both catalysts in the RC1 are much higher than those obtained with the mini-PARR reactor. Furthermore, as showed in Figure 41, the ratio of poly- and mono-branched FA is also dependent on the reactor. An explanation for this behaviour is to be found in the discussion section 4.4.

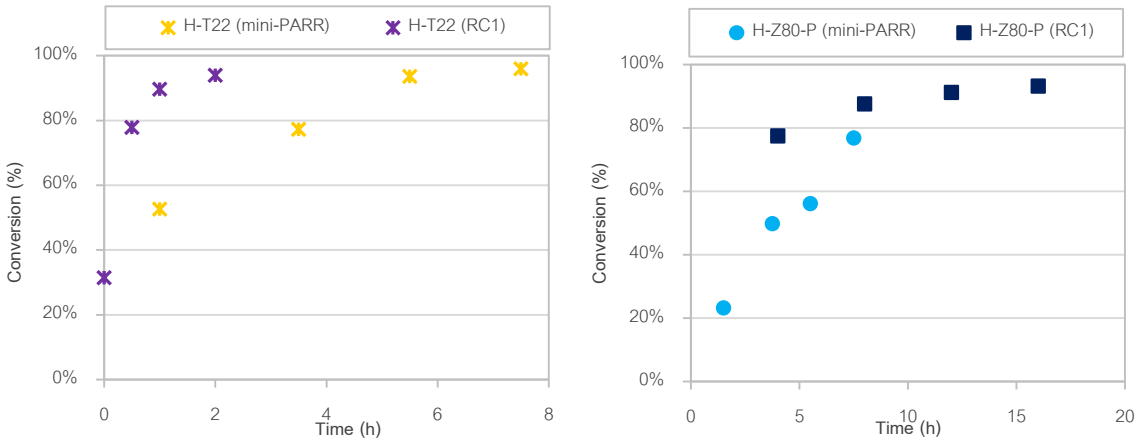

Figure 40: Comparison between RC1 reactor and mini-PARR, when testing H-T22 (left graph) and H-Z80-P (right graph) catalysts for the alkyl-isomerisation of OA. All the reactions were conducted at [..]. % loading.

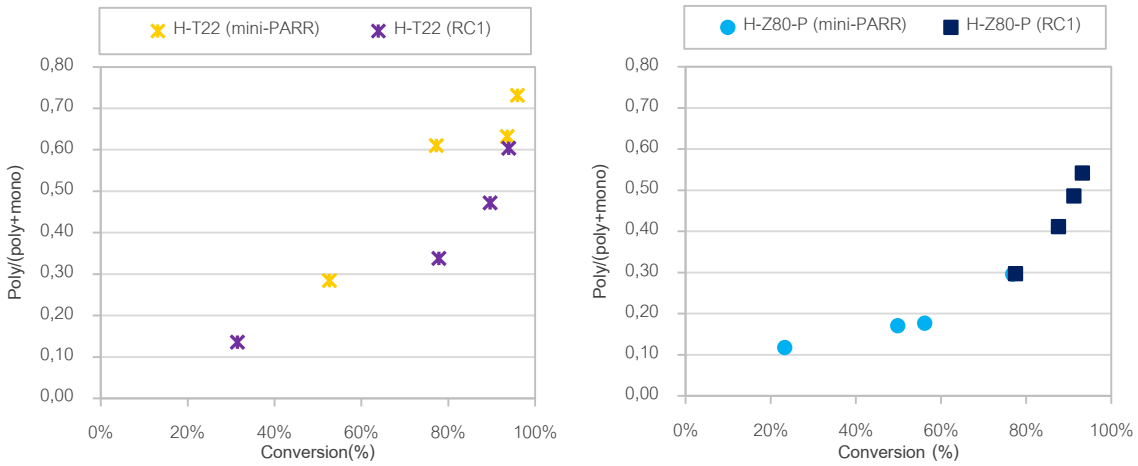

Figure 41: Effect on product branched FA proportions obtained by H-T22 (left graph) and H-Z80-P (right graph) catalysts when tested in different reactors. The conversions of these reactions are represented in Figure 40.

8.3. RC1 experiments for pressure influence

The mini-PARR would generally reach pressures around 4.5-5 bar, but depending on the catalyst, higher pressures were also reached in few cases. On the contrary, in the RC1 reactor, the pressure could be controlled and normally kept at 8 bar. Therefore, it was suspected that this pressure differences might have an influence on the performance of the catalysts obtained with the mini-PARR. The influence of the pressure was therefore investigated with the H-T22 catalyst at a [..]. % loading in the RC1, varying the pressure from 4-5 bar up to 11 bar. However, no significant difference was experienced (see Figure 42). Hence, pressure should not be the parameter that justifies the lower conversions obtained when testing the H-ZSM-5 in the mini-PARR reactor.

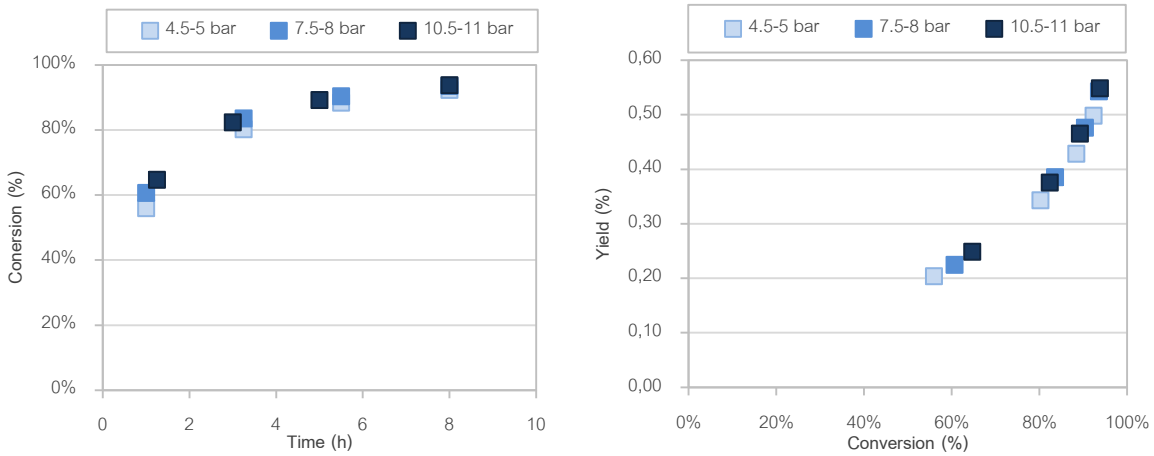

Figure 42: Pressure influence on conversions and branched-FA ratio, tested in the RC1 reactor, with [..]. % loading of the H-T22 catalyst. It is clear that the differences experienced when testing the catalysts in the mini-PARR reactor could not be ascribed to the lower pressures achieved.

8.4. Stirring speed influence on reaction product with mini-PARR reactor

Another parameter that affects the activity of catalyst with diffusion limited problems is the stirring efficiency of the reactants mixture. By testing the same catalyst in a different reactor, higher conversions were in fact obtained see (Appendix 8.2). After excluding pressure related problems (see Appendix 8.3), it was suspected that the reason behind such difference lied in a less

efficient stirring of the mini-PARR setup. The just-received mini-PARR was in fact optimised for alkyl-isomerisation reactions with an H-FER catalyst and it is likely that such catalyst suffers from inefficient stirring less than H-ZSM-5. Therefore, different catalyst tests were performed in the mini-PARR with the H-T22 zeolite at increasing stirring speeds, to verify whether or not increasing stirring speed would affect positively the reaction conversion. The results obtained are reported in Figure 43, compared to the conversion obtained by the same catalyst tested in the RC1 reactor. Clearly, it is shown that the conversion is not influenced by the stirring speed. The ratio between poly-branched and mono-branched yield is also the same for all the three experiments conducted in the mini-PARR.

Nonetheless, it is still believed that a poor stirring efficiency is behind such low conversions obtained by the experiments performed with the mini-PARR. This might be due to the type of stirrer itself. The mini-PARR is in fact provided with a radial impeller with crossed blades, which is placed halfway the reactor height (see Figure 44). With this type of stirrer, the fluid is forced radially toward the vessel walls. Although this should draw the fluid from the bottom and the top of the vessel, it might not be sufficient to avoid the solid catalyst depositing on the bottom of the reactor. On the contrary, the RC1 is provided with 4 axial impellers and a set of baffles, which avoid the formation of a vortex. This setup allows for a much more efficient mixing of catalyst and reactant along the entire height of the vessel.

Only one stirrer was available on site for the mini-PARR reactor, and the catalyst samples were prepared in too small quantities for testing in the RC1; hence, all experiments were performed in the mini-PARR reactor, despite its known inferior characteristics.

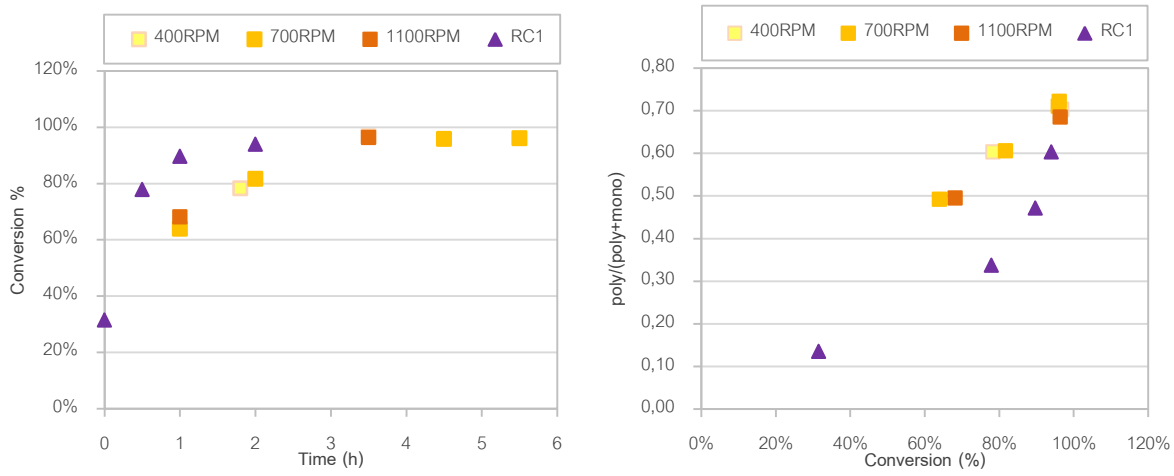

Figure 43: Conversion and the ratio of poly-branched and mono-branched FA yield obtained by testing the H-T22 catalyst in the mini-PARR at different stirring speeds and in the RC1. It is clear that increasing the speed of the stirrer has no effect in enhancing the stirring efficiency in the mini-PARR reactor.

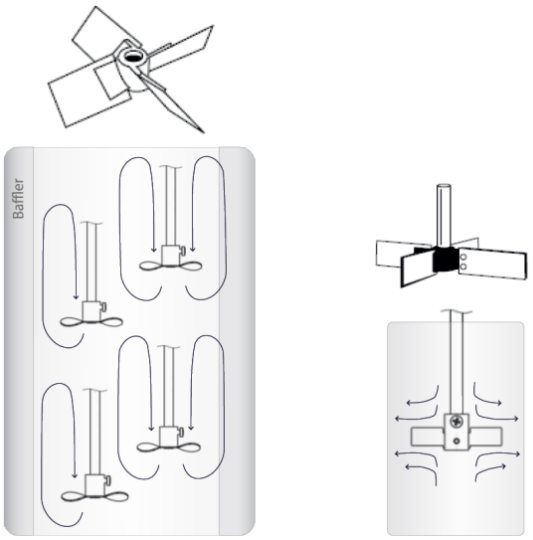

Figure 44: Comparison between the two different types of stirrer found in the RC1, an axial impeller (left) and the mini-PARR reactors, a radial impeller (right). The top figures are a representation of the stirrer blades configuration, while the picture at the bottom represents the approximate flow pattern of the reaction mixture in the two different setups.

Acknowledgements

I would like to thank my supervisor Sophie, for her help and continuous support during these past six months. Her assistance and dedicated involvement in every step throughout this research project were really precious to me. I could not have imagined having a better supervisor.

I would also like to thank Bas, who provided me the opportunity to join the team at Croda as an intern, giving me access to the laboratory facilities and resources. I would also like to thank him for the stimulating discussions, who also opened my mind on how research is conducted outside academic environments.

A special thanks goes to the many people at Croda, who helped me in different ways during my research project. Tanja, for her assistance with the catalytic testing; Marvin, for analysing the innumerable product samples I gave him, with an extreme efficiency. Stephan, for providing the centrifuge which made my life so much easier while preparing my catalyst samples. Cindy and Robbie, for their help with the TGA analyses. Henkjan, for helping me improving my setups. All the other interns and staff members, who made my time here at Croda enjoyable.

Finally, I would like to thank Professor Bert Weckhuysen, who put me in contact with Croda, making this internship possible.